

The Stardalur magnetic anomaly revisited—New insights into a complex cooling and alteration history

C. Vahle^{a,*}, A. Kontny^{a,1}, H.P. Gunnlaugsson^b, L. Kristjansson^c

^a *Geologisch-Paläontologisches Institut, Ruprecht-Karls-University Heidelberg, INF 234, D-69120 Heidelberg, Germany*

^b *Institute of Physics and Astronomy, Aarhus University, Ny Munkegade, DK-8000 Århus C, Denmark*

^c *Institute of Earth Sciences, University of Iceland, Sturlugata 7, Askja, IS-101 Reykjavík, Iceland*

Received 21 December 2006; received in revised form 21 May 2007; accepted 14 June 2007

Abstract

This study provides new rock magnetic and magneto-mineralogical data including Mössbauer spectroscopy of basaltic drill cores from the Stardalur volcanic complex, Iceland, in order to better understand the strong magnetic anomaly, which is caused by an extraordinary high natural remanent magnetization (NRM). NRM and magnetic susceptibility (χ) display a positive linear correlation ($R^2 = 0.81$) and reach very high values up to 121 A/m and 148×10^{-3} SI. Although a Curie temperature of 580 °C and a Verwey transition at about -160 °C is indicative of magnetite, χ - T heating experiments in argon and air atmosphere and thermal demagnetization measurements of NRM revealed a slight cation-deficiency. According to induced remanent magnetization experiments the remanence is carried solely by this low coercive phase. Minor titanomaghemite with a T_C at about 340 °C only occurs in samples with larger oxide grains (20–80 μ m). High vesicle abundances and the exsolution texture of Fe–Ti oxides suggest subaerial extrusion of the lava. A high oxygen fugacity (probably above the NNO buffer) and a low Ti/(Ti + Fe) ratio of the basaltic melt are suggested as a precondition for high concentration of magnetic minerals and therefore high primary TRM. During high temperature oxidation, ilmenite exsolution-lamellae, developed in titanomagnetite, and symplectic magnetite (+ pyroxene) formed by the breakdown of olivine. This secondary magnetite, grown at temperatures above the Curie temperature, increases the primary TRM. Early stage hydrothermal alteration (below about 375 °C) led to maghemitization of (titano)magnetite, clearly indicated by shrinkage cracks and irreversible χ - T curves. During later stage hydrothermal alteration, NRM intensity increased slightly due to the growth of secondary magnetite at lower temperatures (about 250–300 °C). This hydrothermally formed magnetite acquired only a low CRM but increased magnetic susceptibility significantly. According to our results it is suggested, that hydrothermal alteration does not necessarily lower remanent magnetization, but contributes to an increase in magnetization. The interplay of the three factors melt composition, small grain sizes of secondary magnetite due to decomposition of silicates and new formation under hydrothermal conditions caused the strong magnetic anomaly at the surface.

© 2007 Elsevier B.V. All rights reserved.

Keywords: Magnetic anomaly; Rock magnetism; NRM; Magnetite; Maghemite; Basalt alteration

1. Introduction

Aeromagnetic surveys of Iceland have revealed different types of magnetic anomalies. Mainly, they are aligned subparallel to currently active or extinct spreading zones. The resulting magnetic lineations are related

* Corresponding author.

E-mail address: cgv@gmx.de (C. Vahle).

¹ Present address: Geologisches Institut, Universität Karlsruhe (TH), Hertzstr. 16, D-76187 Karlsruhe, Germany.

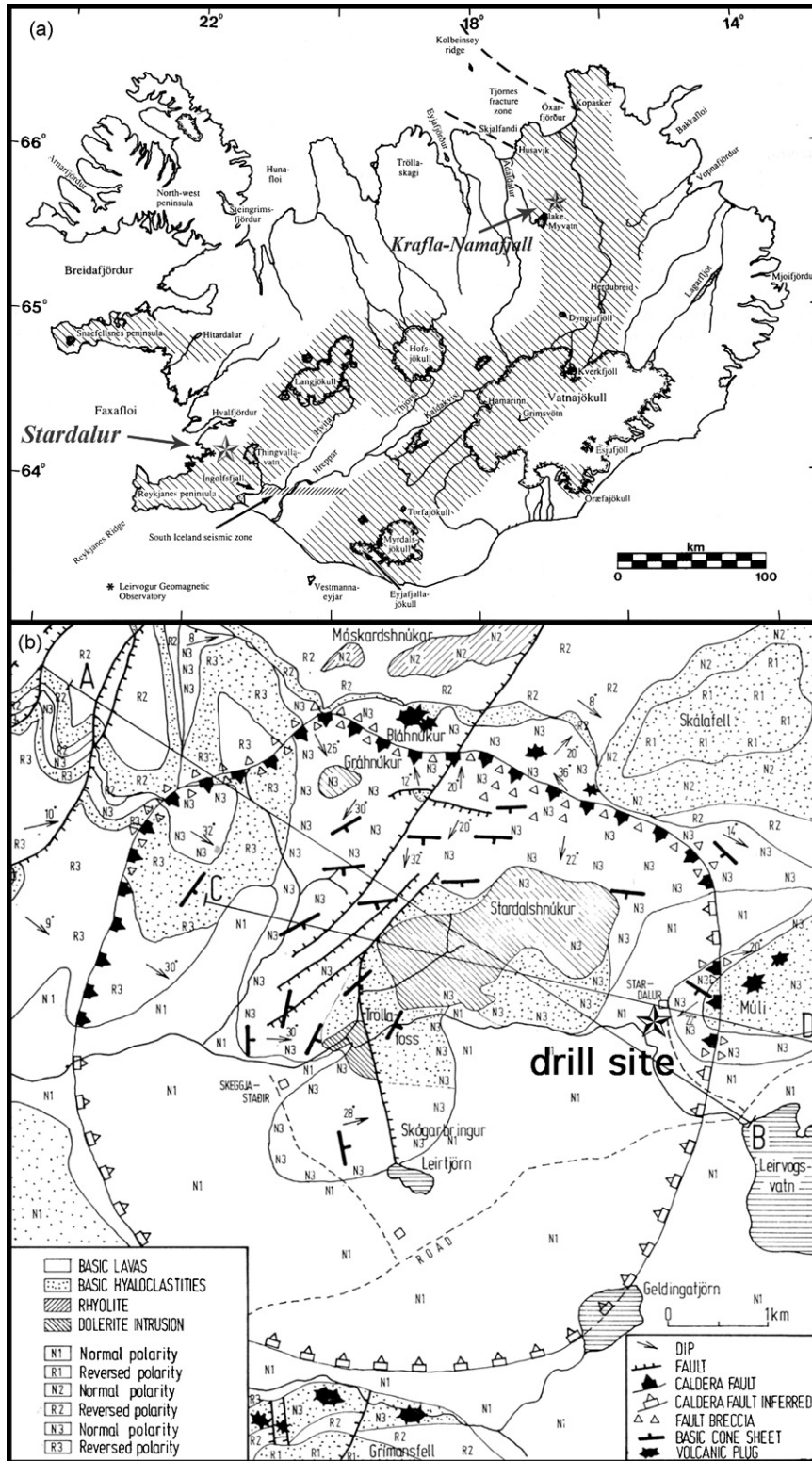


Fig. 1. (a) Location of the Stardalur volcanic complex and present zones of volcanism and crustal spreading (shaded areas) in Iceland (additionally, the glacier (jökull) outlines are shown; modified from Jonsson et al., 1991); (b) geological map with location of the drill site (modified from Fridleifsson and Kristjánsson, 1972, lines A–B and C–D refer to cross-sections described therein).

to tilted blocks and/or changes in magnetic polarity (Jonsson et al., 1991). Additionally, several localized magnetic anomalies of 5–10 km in size are associated with volcanic centers. Some have high magnetic intensity (positive anomaly in a negatively polarized area), others show magnetic lows (negative anomaly surrounded by strong positive anomaly), like in the Krafla–Namafjall area (Fig. 1a). The latter type seems to be related to hydrothermal activity in geothermal fields.

The strongest of the localized positive magnetic anomalies is observed at the Stardalur volcanic complex, 20 km NE of Reykjavik (Fig. 1, Fridleifsson and Kristjansson, 1972). According to unpublished data from Th. Sigurgeirsson from an aeromagnetic survey at 100–200 m above ground, the maximum field of the Stardalur magnetic anomaly is 59 μT , whereas the neighboring area gives only 51 μT . The Stardalur volcanic complex is of Olduvai age (~ 1.8 Ma) and consists of a 6.5 km caldera, cone-sheet swarm, sills and a laccolithic body. At the northern rim of the caldera, intensive fracturing enabled hydrothermal activity. The volcanic complex is embedded into thick successions of basaltic lava flows of Quaternary age, intercalated with hyaloclastite ridges and glacial deposits (Fridleifsson, 1973).

In the years 1969–1970, a 200 m deep borehole was drilled into the area of maximum field intensity of the Stardalur magnetic anomaly. A first rock magnetic characterization of these drill cores was done by Fridleifsson and Kristjansson (1972). The average natural remanent magnetization (NRM) was 61 A/m. This is about 10 times higher than the average of other Icelandic Quaternary basalts (Kristjansson, 1970). From thermomagnetic measurements done in air, the authors found magnetite resulting from high temperature oxidized titanomagnetite, which is in some cases subsequently oxidized to maghemite. Due to stable NRM directions and no time dependence they excluded a strong viscous overprint. Furthermore, the small scattering of the NRM inclination ($81 \pm 4^\circ$) pointed to a short time interval of lava emplacement (~ 2000 years). Based on saturation remanence and susceptibility data, Fridleifsson and Kristjansson (1972) estimated the magnetite content to be 2.5 vol.%. They concluded this high magnetite content to be one reason for the unusually strong magnetic anomaly. Additionally, they assumed a high paleomagnetic field intensity of $93 \pm 6 \mu\text{T}$ at the time of NRM acquisition (actual Earth magnetic field at Stardalur is 52 μT , IGRF-10). It was also suggested, that rather small grain sizes resulting from rapid cooling or oxidation contribute to high NRM.

Helgason et al. (1990) inferred similar conclusions and suggested an additional self-amplification effect of the magnetic field due to hydrothermal reheating from

below. The oxidized titanomagnetite (magnetite with Curie temperature of 580 °C) shows still ferromagnetic behavior despite elevated temperatures due to hydrothermal heating and therefore increases the local magnetic field. According to Mössbauer spectra they found neither maghemite nor Ti in the magnetic phase, only pure and homogeneous magnetite. But Helgason et al. (1990) stated already “that the key of the riddle lies in the alteration process”.

Using Mössbauer spectra and scanning electron microscopy (SEM) Gunnlaugsson et al. (2006) have shown the influence of oxidized olivine on magnetic properties of olivine basalt. According to their study, submicroscopic single-domain magnetite, which formed by oxidation of olivine, increases NRM. Therefore, the NRM of basalts containing olivine could be an order of magnitude higher than that of olivine-free basalts. Furthermore, Stardalur samples have been found to have a rather high Fe-content of ~ 12 wt.% Fe (Steinþorsson and Sigvaldason, 1971), with an unusually large proportion of Fe situated in magnetite (about 30% of the area of the Mössbauer spectra, 5–10% is more usual; Helgason et al., 1990; Gunnlaugsson et al., 2003).

According to these previous studies following factors seem to account for the unusually high magnetizations of the Stardalur rocks: (1) small grain size, (2) high temperature oxidized titanomagnetite, resulting in almost pure magnetite, (3) magnetite oxidized from olivine and (4) higher (local) paleomagnetic field intensity. Although it seems that probably all of these factors contribute, the geological processes that led to the anomalously high magnetization of the Stardalur rocks are not fully understood. Although Mössbauer studies revealed pure magnetite as carrier of the magnetic properties (Helgason et al., 1990; Gunnlaugsson et al., 2003, 2006) it is not fully clear up to now how the magnetite has actually formed and how the textural relations are. Therefore, we combined rock magnetic and magneto-mineralogical methods, in addition to thermomagnetic experiments, to find further clues to this extraordinary high magnetization. A better understanding of the Stardalur anomaly may be an analogue for extraterrestrial magnetic anomalies, e.g. observed on Mars, where strong crustal anomalies are attributed to a high crustal remanence (e.g. Acuña et al., 1999). Models suggest magnetic rocks of tenths of km thickness with remanent magnetization up to ~ 20 A/m (Purucker et al., 2000).

2. Sample material and methods

We investigated drill cores of the 200 m deep Stardalur borehole (Fig. 1b) drilled in the years 1969–70

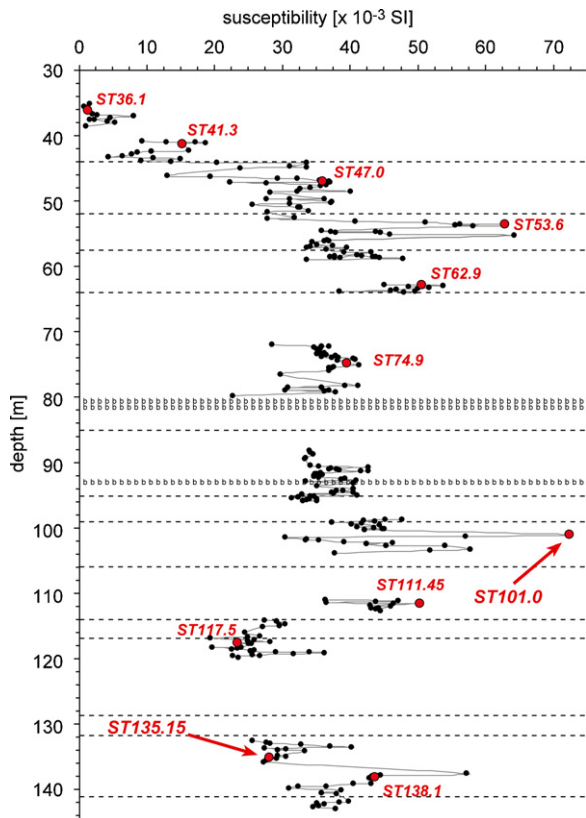


Fig. 2. Susceptibility profile of the Stardalur core and location of samples (b, brecciated zone). The lithological boundaries are picked from the lithological profile described in Fridleifsson and Tomasson (1972).

(see above). The drill core revealed about 45 m of fresh olivine tholeiitic lava flows and tuffs with low magnetic intensity. Below that depth until at least 140 m, strongly magnetic early Quaternary lavas follow (Fridleifsson and Kristjansson, 1972). Between 35 and 143 m we measured magnetic susceptibility on full cores (Fig. 2) using a hand-held kappameter (KT-5) from Geofyzika (now AGICO company). The measurement sensitivity is 1×10^{-5} SI based on frequency changes of the operating coil (10 kHz). The average distance between single measurements was ~ 21 cm, whereas not the entire core was measured because of missing sections. Based on the susceptibility profile we selected representative samples, which reflect the observed susceptibility variations. From these samples, standard cylindrical specimens (2.5 cm in diameter, 2.1 cm high) were prepared for different rock magnetic investigations.

The magnetic susceptibility (χ) was measured in the laboratory on these specimens using KLF-3 susceptometer of Geofyzika (now AGICO company) at 30 A/m and 2000 Hz. The reliability and significance of routine susceptibility measurements on drill cores using

a hand-held kappameter were compared with laboratory measurements. This test gives a linear relationship between both these methods with a high correlation coefficient ($R^2 = 0.99$, $n = 11$), whereas a general shift towards lower values for the hand-held kappameter measurements can be observed ($y = 0.551 \times -0.497$). Using hand-held kappameter measurements to reveal the pattern of magnetic susceptibility one must be aware that the hand-held kappameter values are lower than those measured on standard cylindrical specimens.

For the temperature dependence (-194 to 0 and from room temperature to 700°C) of magnetic susceptibility ($\chi-T$) a KLY-4S kappabridge (working with 300 A/m and 875 Hz) combined with a CS-L/CS-3 apparatus (AGICO company) was used. Heating/cooling rates range between $3-4$ and $11-14^\circ/\text{min}$ for the low temperature and high temperature run, respectively. The high temperature runs were performed in an argon atmosphere in order to avoid mineral reactions with oxygen during heating (flow rate of 110 ml/min). Some samples were also measured in an air flow of the same rate. The raw data were corrected for the empty cryostat/furnace and normalized to the susceptibility magnitude at 0°C . The Néel or Curie temperature (T_N or T_C) was determined graphically using the reciprocal susceptibility according to the suggestions of Petrovsky and Kapicka (2005).

Measurements of remanent magnetization were done with a JR5A spinner magnetometer (AGICO company). For stability tests, alternating field demagnetization (AF demagnetization) was performed in peak fields up to 160 mT with a MI AFD 1.1 from Magnon International. Stepwise thermal demagnetization up to 700°C was done with the Thermal Demagnetizer MMTD1 (magnetic measurements). Isothermal acquisition of remanence (IRM) was measured using a commercial power supply unit connected with a coil for fields up to ca. 90 mT. For selected samples IRM was applied at fields of 1.25 T with an ASC Scientific Impulse Magnetizer (IM-10-30) and subsequent stepwise thermal demagnetization was performed with an ASC Scientific Thermal Demagnetizer (TD-48) at the Laboratory for Natural Magnetism, ETH-Zurich.

Oxide textures were characterized using reflected light and scanning electron microscopy in backscatter mode (LEO 440). Mineral chemical data were obtained by electron microprobe (CAMECA SX51) at the Institute of Mineralogy in Heidelberg. Standards used were periclase (Mg), Al_2O_3 (Al), wollastonite (Si), TiO_2 (Ti), Cr_2O_3 (Cr), rhodonite (Mn), and hematite (Fe). The raw data were corrected with the PAP algorithm of Pouchon and Pichoir (1984). An acceleration voltage of 15 kV and a sample current of 20 nA were used.

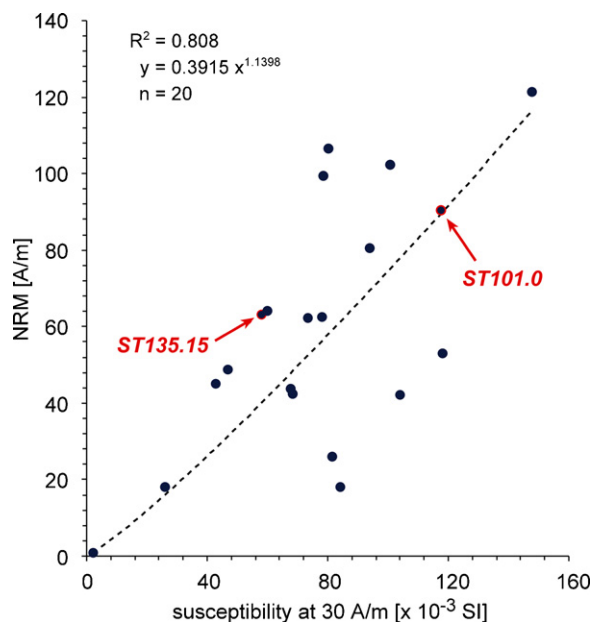


Fig. 3. Magnetic susceptibility (measured at field amplitude of 30 A/m) vs. natural remanent magnetization (NRM) of all sample cylinders.

Mössbauer spectra (done at the Institute of Physics and Astronomy of Aarhus University) were recorded in transmission geometry at room temperature using 10–25 mCi $^{57}\text{Co}:\text{Rh}$ sources mounted on conventional drive systems. Isomer shifts (δ) and velocity are given relative to the center of the spectrum of $\alpha\text{-Fe}$.

3. Results and interpretation

Table 1 summarizes the rock magnetic parameters from the basaltic samples marked in Fig. 2. The magnetic susceptibility pattern agrees quite well with lithological boundaries indicating changes in cooling and alteration history. Natural remanent magnetization (NRM) versus magnetic susceptibility (χ) of all specimens displays a positive linear correlation with $R^2=0.81$ (Fig. 3). NRM and χ reach very high values up to 121 A/m and 148×10^{-3} SI, respectively. These high values suggest a high content of opaque minerals. A positive correlation between the NRM and the estimated volume percent of the opaque minerals of some polished sections (see below) confirms this assumption ($R^2=0.69$; $n=7$). An even better correlation with $R^2=0.75$ has been found between magnetic susceptibility and the volume percentage of the opaque minerals.

Average values calculated for the strongly magnetic samples below 43 m are 62.6 ± 23.8 A/m and $82.4 \pm 24.4 \times 10^{-3}$ SI, respectively. These values fit

quite well to the average NRM intensity of 61 A/m for the Stardalur rocks given by Fridleifsson and Kristjansson (1972). A comparison with NRM intensities and susceptibilities of other Quaternary Icelandic rocks (about 10 times less magnetic, see Kristjansson, 1970) and of own unpublished data from surface rocks of the Reykjanes peninsula (13.8 ± 6.2 A/m and $10.2 \pm 4.0 \times 10^{-3}$ SI; recent lava flows from fissure eruptions, shield volcanoes and pillow lava, all younger than 20,000 years) emphasizes the unusually high values for the Stardalur basalts. The Königsberger ratio, Q -factor (ratio between remanent and induced magnetization), ranges between 7.5 and 30.4, clearly indicating the predominance of remanent magnetization over induced magnetization. Component analyses revealed only one stable characteristic remanence direction contributing to the NRM. In the following sections, we give a rock magnetic and magneto-mineralogical characterization to better understand the nature of this extraordinary magnetic behavior.

3.1. Microscopic observations

According to the lithological descriptions given in Fridleifsson and Tomasson (1972) the units below about 45 m are altered olivine tholeiitic basalt. In the lower part of this section at ~ 140 m depth, zeolite, montmorillonite and chlorite are reported. Based on our own macroscopic observations the main part of the core from 44 down to 144 m consists of differently strong altered fine-grained basalts with local carbonate and quartz fillings along cracks and veins. Two breccia zones at 81 and 93 m, respectively, intercalate these basalts (see Fig. 2). In the lowermost part (ST138.1) many vesicles (about 15 vol.%) with a diameter of 1–5 mm point to subaerial extrusion of the lava. These vesicles are filled with white and green minerals, probably the above described zeolite, montmorillonite and chlorite.

According to microscopic observations, the main silicates are subhedral (200–500 μm) or columnar plagioclase laths (60–800 μm in size). No olivine is observed, but in some samples altered areas of 60–300 μm in size are found consisting of phyllosilicates (predominantly chlorite), which could have been former olivine. According to their brown and greenish color, some of these altered areas could be iddingsite (submicroscopic mélange of goethite, chlorite and phyllosilicates), a low to intermediate temperature alteration product of olivine (Baker and Haggerty, 1967). But also symplectic magnetite has been observed at some places (Fig. 4a), which is assumed to be a high temperature oxidation product of olivine. Based on heating experiments of olivine basalt from different localities,

Table 1
Rock magnetic properties of the Stardalur samples (no average values, data of single cylinders)

Sample	Depth [m]	Lithology	NRM [A/m]	Q	χ (30 A/m) [10^{-3} SI]	MDF [mT]	SIRM [A/m]	opaque mineral content [vol.%]
ST36.1	36.1	Tuff	0.6	7.5	2.1	27	–	–
ST41.30	41.3	Hyaloclastite	17.7	16.4	25.9	32	883	6
ST47.00	47.0	Basalt	42.0	14.8	68.3	23	–	–
ST53.60	53.6	Basalt	52.6	10.7	118.0	14	1941	11
ST62.90	62.9	Basalt	80.3	20.5	93.9	24	3077	10
ST74.90	74.9	Basalt	62.2	19.2	78.0	22	–	–
ST101.00	101.0	Basalt	90.5	18.4	118.0	18	2489	15
ST111.45	111.5	Basalt	25.6	7.5	81.5	13	–	8
ST117.50	117.5	Basalt	48.3	24.8	46.8	25	–	7
ST135.15	135.2	Basalt	63.0	26.0	58.3	34	2414	9
ST138.10	138.1	Basalt	99.2	30.4	78.5	23	–	–

NRM: natural remanent magnetization, Q : Königsberger ratio (calculated with a field intensity of 41.6 A/m), χ (30 A/m): magnetic susceptibility measured at 30 A/m, MDF: median destructive field, SIRM: saturation isothermal remanence at 1.25 T.

Haggerty and Baker (1967) stated that olivine oxidizes to magnetite + enstatite or hematite + forsterite depending on temperature and oxygen fugacity.

Additionally to clinopyroxene and plagioclase, opaque minerals, carbonate, quartz and chlorite occur in the Stardalur drill cores. Following opaque minerals have been identified:

- titanomagnetite: dendritic, cruciform, skeletal to euhedral grains, <1 μm and up to 130 μm in size;
- ilmenohematite: elongated skeletal to subhedral grains of 12–100 μm ;
- titanite: as alteration product of ilmenohematite and titanomagnetite;
- sulfide phases: pyrite and chalcopyrite, subhedral grains up to 300 μm ;
- magnetite: net-like replacement products and vein fillings.

The total abundance of the opaque minerals was estimated from thin section observations and ranges between 6 and 15 vol.% (see Table 1). The opaque mineral assemblage is strongly dominated by titanomagnetite, which has been proved by the application of a ferrofluid (see, e.g. Kletetschka and Kontny, 2005). Because the ferrofluid covers only magnetic phases like titanomagnetite and magnetite, the coating with ferrofluid enables the discrimination of, e.g. ilmenite and magnetite. Ilmenohematite and especially titanomagnetite show different textures and grain size populations, indicating different cooling and crystallization histories of the basalts. Almost all titanomagnetite shows ilmenite exsolution-lamellae, resulting from high temperature oxidation (Fig. 4b). Some ilmenohematite shows lenses of rutile

and probably hematite spots. In some cases sandwich-types are present. These textures are in accordance with the oxidation stages C3/4 and R2-4 given by Haggerty (1991). Additionally, shrinkage cracks and a mottled texture of the grains point to some degree of maghemitization of titanomagnetite (Fig. 4c). The sulfide phases are of secondary origin, because they are often found along cracks and veins and are associated with carbonate and quartz (Fig. 4d). Some pyrite grains are altered and replaced by magnetite (Fig. 4d) suggesting a change in fluid chemistry or physico-chemical conditions. Therefore, magnetite is not only produced by oxyexsolution of titanomagnetite or breakdown of olivine but also by secondary growth. This magnetite shows a net-like porous texture and small, 8–20 μm sized euhedral cubes (Fig. 4d). Fig. 4e shows the growth of such secondary magnetite along a $\sim 20 \mu\text{m}$ wide vein. The marked area in Fig. 4e is shown with higher magnification in Fig. 4f. On the left side of the photograph, areas possibly representing ilmenite-lamellae can be observed. These areas seem to be relics of exsolved titanomagnetite, where both, titanomagnetite and ilmenohematite have been dissolved. The alteration products consisting of dark grey areas with needle-like crystals are too small to be reliably analyzed, but the data are very similar to an ilmenite composition with up to 9.4 wt.% MnO. For comparison, the homogeneous ilmenohematites have MnO contents of 1.62–2.32 wt.%. In some cases the ilmenite-lamellae in titanomagnetite are dissolved and partly replaced by titanite leaving behind a “ghost” texture (Fig. 4b). Also some titanomagnetite is dissolved, which probably supplied the material for the growth of secondary magnetite (Fig. 4d–f; see also Section 4). These microscopic observations imply that the secondary magnetite must be

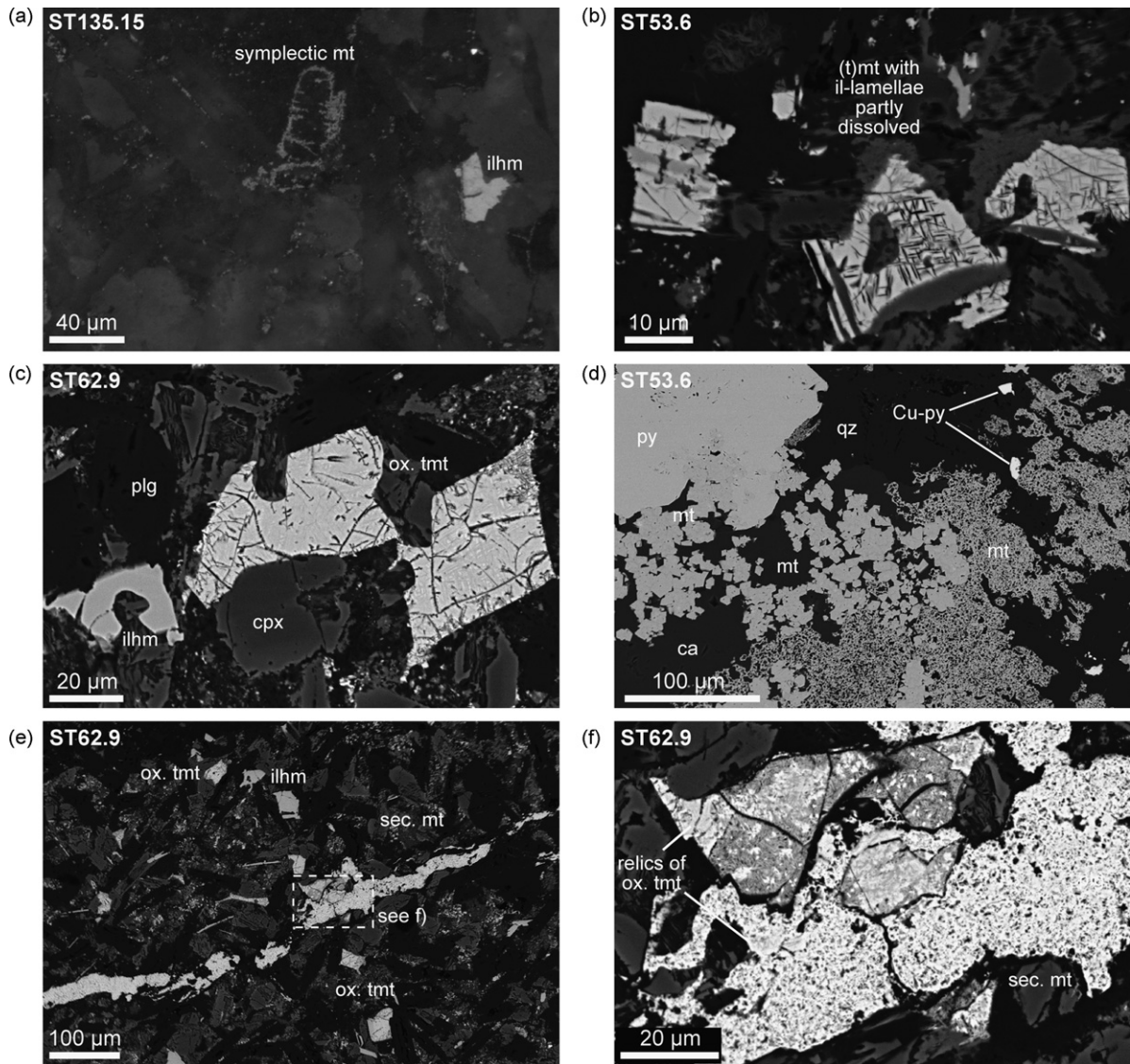


Fig. 4. Oxide textures of the Stardalur basalts show the processes affecting the magnetic minerals ((a) reflected light, in oil immersion and coated with ferrofluid, (b–f) SEM images taken in backscatter mode): (a) symplectic magnetite around former olivine during high temperature oxidation; (b) ilmenite-lamellae in titanomagnetite host (partly with dissolved ilmenite) during high temperature oxidation; (c) maghemitized titanomagnetite with shrinkage cracks working as pathways for hydrothermal fluids altering the Fe–Ti oxides; (d) secondary pyrite (py) and magnetite (mt), associated with carbonate (ca), quartz (qz) and chalcopyrite (Cu-py); (e) secondary magnetite crystallized along veins; (f) the area marked in (e) with higher magnification showing relics of oxidized titanomagnetite surrounded by net-like, porous secondary magnetite (tmt: titanomagnetite, ilm: ilmenohematite, plg: plagioclase, cpx: clinopyroxene, ox: oxidized).

considered for the interpretation of the high NRM intensity and χ -values.

For the strongly magnetic lower part of the Stardalur profile two groups of oxide textures can be distinguished. Group 1 (Fig. 5a and b) is characterized by rather dendritic and cruciform titanomagnetite with small grain sizes of 5–10 μm (max. 20 μm in length). These grains show exsolution textures typical for high

temperature oxidation and shrinkage cracks indicating maghemitization. The high opaque mineral content of up to 15 vol.% is reflected in the highest values for NRM intensity and χ (see also Fig. 3). This texture is characteristic for rapid cooling as observed in submarine basalts or marginal parts of subaerial lava flows (e.g. Kontny et al., 2003). Vesicles of up to 1 mm are filled with predominantly chlorite, associated with

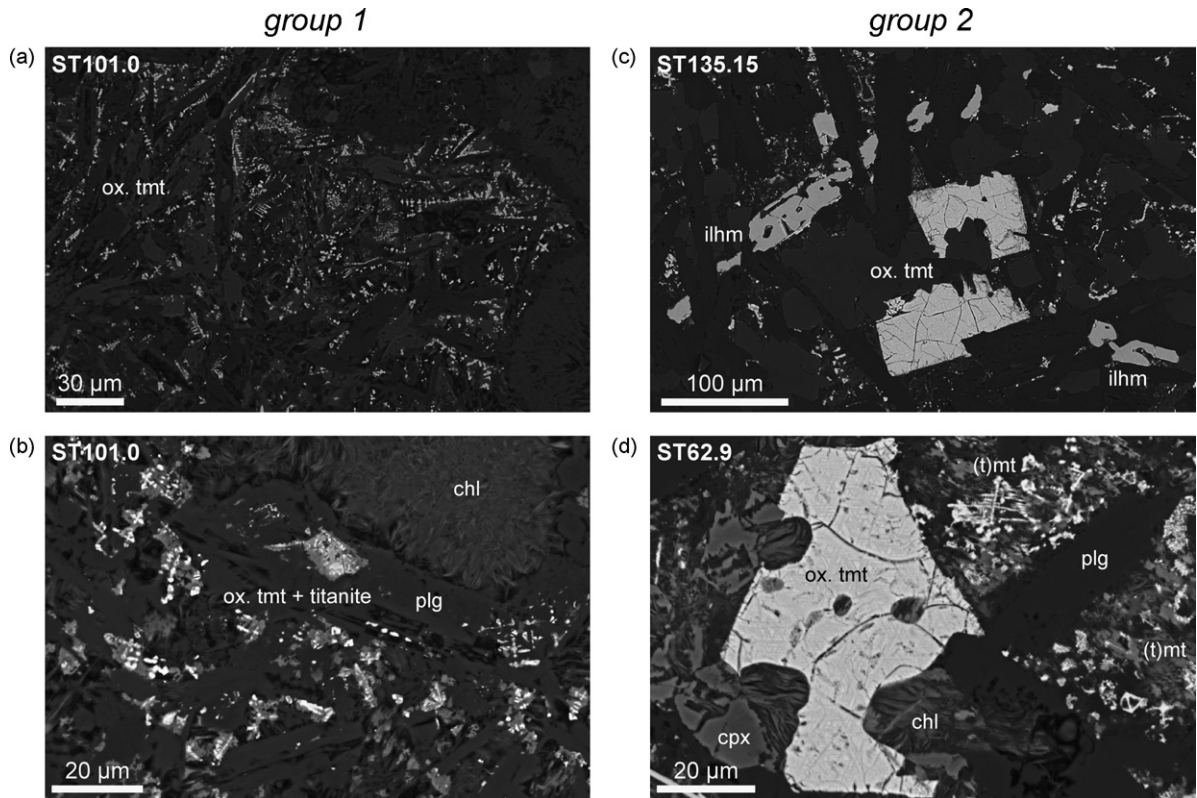


Fig. 5. Different oxide textures of representative samples for group 1 and 2 (SEM images in backscatter mode): group 1 (a and b, ST101.0): skeletal to dendritic Fe–Ti oxides of small grain size comparing to group 2 with a bimodal grain size spectrum with skeletal to euhedral and dendritic crystals for ST135.15 (c) and ST62.9 (d; tmt: titanomagnetite, ilhm: ilmenohematite, plg: plagioclase, chl: chlorite, cpx: clinopyroxene, ox: oxidized).

pyroxene + quartz \pm magnetite and carbonate + titanite, respectively. Whereas no ilmenohematite was found in this group, the second group clearly contains ilmenohematite (Fig. 5c). The ilmenohematite grain sizes range between 12 and 80 μm with partly elongated skeletal shapes. The titanomagnetite shows a dense network of ilmenite-lamellae, and shrinkage cracks (Fig. 5c and d). This second group shows a distinct bimodal grain size population ranging from dendritic, cruciform to xenomorphic grains in the groundmass with less than 10 μm size to subhedral and euhedral grains with 20–80 μm in size (Fig. 5d).

In contrast to the strongly magnetic lower part of the profile the upper part at the top (around ST36.1) with very low magnetic susceptibilities (Fig. 2) consists of a greenish to pale-grey, soft, tuffaceous rock. Below this tuffaceous rock a zone ($\sim 4\text{ m}$ thick) of dark greenish to grey rocks with clasts less than 4 mm in size follows with low to intermediate χ -values ($4\text{--}20 \times 10^{-3}$ SI). Microscopic observations revealed altered, rounded glass shards (palagonite) of up to 1 mm in size surrounded by carbonate and quartz. The boundaries of the

glass shards are lined with abundant opaque phases of up to 20–30 μm size, but mostly $< 10\ \mu\text{m}$, with irregular shape. With respect to the χ -values, these are most likely titanomagnetite with very low to no Ti content. The ferrofluid is attracted to almost all opaque phases in this rock. Additionally some sulfide phases (up to 40 μm) occur, of which some are found in titanomagnetite and therefore, could have crystallized first and acted as nuclei for the Fe–Ti oxide.

3.2. Alternating field and thermal demagnetization

Alternating field (AF) at room temperature and in air atmosphere and thermal demagnetization experiments in air atmosphere were done to get information about the stability of remanence and the kind of mineral(s) carrying the remanence. Generally, the median destructive field (MDF, the field that is necessary to remove half of the NRM) of the Stardalur basalts ranges between 13 and 34 mT (Table 1). In comparison with AF demagnetization experiments done on crushed annealed magnetite (with TRM, thermoremanent magnetization, of 0.1 mT,

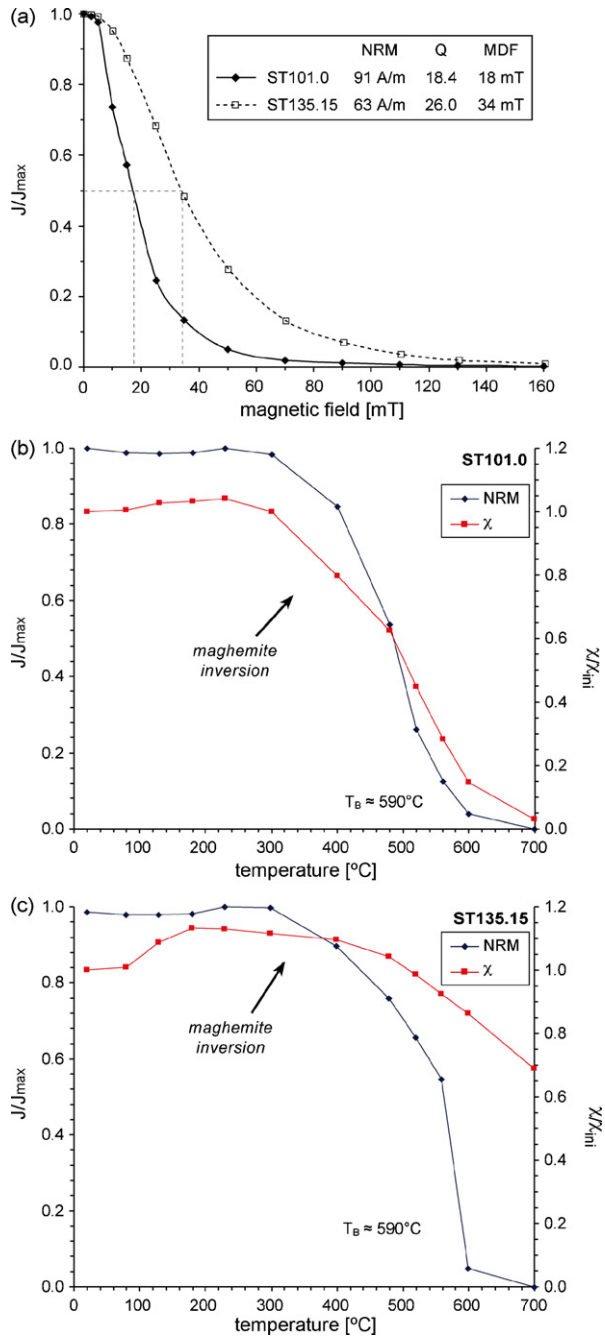


Fig. 6. (a) Alternating field demagnetization of ST101.0 and ST135.15 with median destructive field (MDF); (b and c) thermal demagnetization of NRM with accompanying χ -measurement for both samples.

Dunlop et al., 2004), the Stardalur rocks show similar demagnetization behavior like the samples in the pseudo-single-domain to multi-domain size range (compare Fig. 6a in this publication with Figs. 2 and 5 in Dunlop et al., 2004). According to microscopic observations (see

above) and temperature dependent susceptibility measurements (see Fig. 8) two groups of magnetic behavior have been distinguished, which will be described in the following using representative samples ST101.0 and ST135.15. Fig. 6 presents AF and thermal demagnetization curves for these two samples.

Stepwise AF demagnetization (Fig. 6a) shows a continuous decrease of magnetization with increasing magnetic field amplitude, but the derived MDF is significantly higher in sample ST135.15. In regard to the oxide textures of the samples (ST101.0 shows much smaller grain sizes than ST135.15) this result may be surprising. But the large oxidized titanomagnetite grains in ST135.15 contain many ilmenite-lamellae developed during high temperature oxidation subdividing the originally homogeneous titanomagnetite grains. This type of texture can cause MDF values in the range around 30–40 mT, as described, e.g. for oxidized subaerial basaltic lava of Hawaii (Kontny et al., 2003).

Thermal demagnetization curves for the representative samples (Fig. 6b and c) show almost a constant course of magnetization until 300 °C. After heating to higher temperatures NRM intensity decreases continuously resulting in a blocking temperature (T_B) of $\sim 590^\circ\text{C}$. A very small portion of the NRM still appears above 600 °C and vanishes at 700 °C (Figs. 6 and 7). A high T_B of more than 590 °C, typical for a maghemite-like phase, can be assumed for some samples studied by Fridleifsson and Kristjansson (1972), who found T_C higher than 590 °C using strong-field thermomagnetic measurements. After each demagnetization step, we measured χ to check if chemical changes occurred during heating. For sample ST101.0 a very strong decrease in susceptibility has been observed. Less than 10% of the initial values remain after the final heating step at 700 °C. This observation clearly indicates, that the magnetic phase, which should be most likely magnetite according to its T_B at 590 °C, is not stable during heating. Based on own unpublished measurement of synthetic and natural magnetite, this is unusual for pure stoichiometric magnetite, and therefore we assume that the magnetite is cation-deficient and transforms to hematite during heating. While almost 50% of the NRM is lost already at 480 °C for ST101.0, thermal demagnetization of ST135.15 revealed a different behavior with a stronger temperature resistance. Indeed the blocking temperatures are the same but 50% of the NRM is retained until 560 °C. Above that temperature, a steep decrease can be observed. Furthermore, less alteration during heating is indicated by the susceptibility, which is 2/3 that of the initial value after heating to 700 °C. While sample ST101.0 shows a change in color from grey to deep red, in sam-

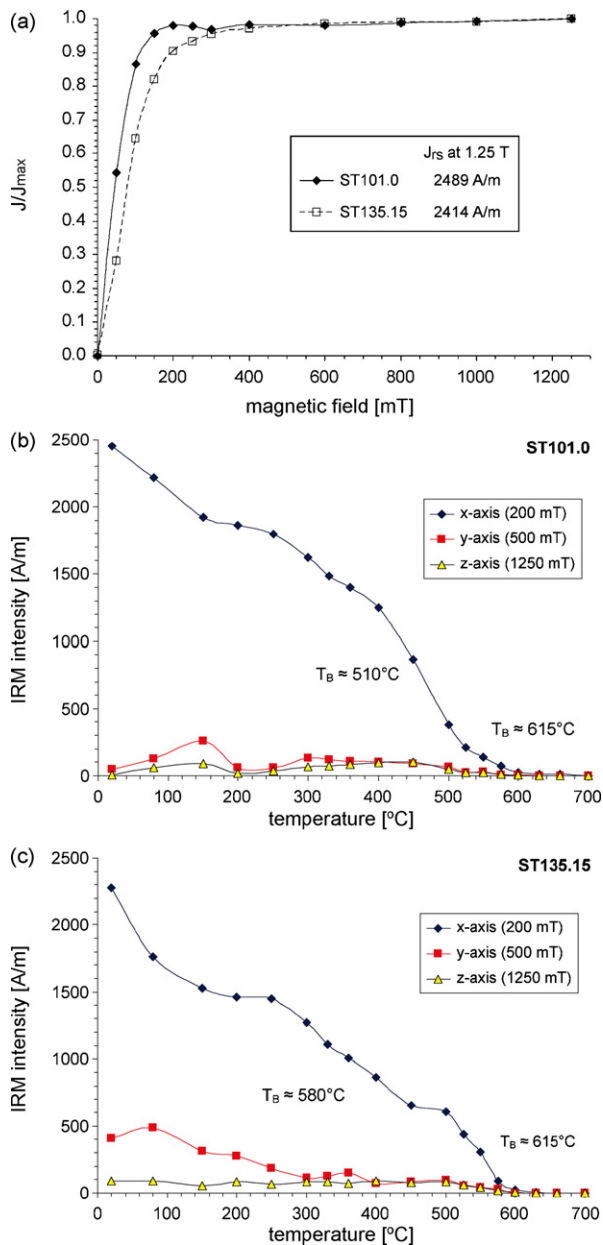


Fig. 7. (a) Acquisition of isothermal remanent magnetization (IRM) for ST101.0 and ST135.15 (J_{RS} : saturation remanence); (b) and c) thermal demagnetization of saturated IRM after the Lowrie method (Lowrie, 1990): first 1.25 T are applied along the z-axis, then 500 mT parallel to the y-axis and finally 200 mT in direction of the x-axis to identify contributions of minerals with different coercivity.

ple ST135.15 only some areas have changed to red color after heating above 600 °C. These observations are corroborated by the Mössbauer findings, which show less alteration of the ST135.15 sample. At least three explanations are conceivable up to now for this difference: (1) ST101.0 exhibits a stronger degree of cation-deficiency

resulting in stronger thermal instability, (2) ST135.15 is less sensitive to maghemitization because some parts of the oxidized titanomagnetite grains resist oxidation due to the large grain size, and (3) ST101.0 contains more magnetite derived from oxidation of olivine, this magnetite has lower MDF and less thermal stability than magnetite derived from exsolution of titanomagnetite. Further experiments have been conducted to unravel these questions.

3.3. IRM acquisition and thermal demagnetization of three-component IRM

The acquisition of isothermal remanent magnetization (IRM) up to 1.25 T at ambient temperature gave similar results as the AF demagnetization curves. For ST135.15 higher field amplitudes are needed to impress a magnetization: ST101.0 is saturated already at 200 mT, while a magnetic field of at least 400 mT is needed for ST135.15 (Fig. 7a). This is again a factor of two as already observed for the MDF values. Despite the difference in NRM intensity, the saturation remanence is nearly the same for both samples.

Thermal demagnetization of three-component IRM is used to identify the influence of different coercive minerals on the magnetization (Lowrie, 1990). In this experiment, the maximum field of 1.25 T is applied parallel to the z-axis of the sample cylinder, then 500 mT along the y-axis and the lowest field of 200 mT in direction of the x-axis. Subsequent thermal demagnetization of IRM with respect to the axis of applied field is shown in Fig. 7b and c. For both samples a similar behavior can be observed. The initial decrease until 150 °C is attributed to some kind of viscous remanent magnetization, which would disappear after some time of relaxation (A. Hirt, personal communication, 2006). At higher temperatures for both samples a more or less continuous decrease in IRM intensity, typical for multi-domain magnetite, can be observed with T_B of ~ 510 and 615°C for ST101.0 and 580 and 615°C for ST135.15, respectively. The IRM is almost entirely carried by the low coercive phase (x-axis, 200 mT) suggesting that there is no contribution of an ilmenohematite phase or another high coercive mineral like, e.g. goethite to the remanent magnetization of the Stardalur rocks. Only for ST135.15 a small influence of a higher coercive phase is seen due to higher IRM intensity of y-axis. This observation is in agreement with the IRM acquisition curve (Fig. 7a) and is probably related to the intense exsolution texture of the titanomagnetite grains and/or the occurrence of cation-deficient (titano)magnetite (Özdemir et al., 1993).

3.4. Temperature dependent magnetic susceptibility

Temperature dependent magnetic susceptibility (χ - T curves) is a quick and very sensitive method for the identification of magnetic phases. Furthermore, the degree of reversibility of the heating and cooling run allows an estimate of phase changes, which can be interpreted in terms of the stability of the original magnetic phases.

Representative χ - T curves for several selected samples are shown in Fig. 8. For the hyaloclastite sample (ST41.3) from the top of the profile a peak in susceptibility at -159°C is observed in a first low temperature run (Fig. 8a), which can be related to the Verwey transition of magnetite. Usually, this crystallographic transition from monoclinic to cubic symmetry occurs in the temperature range -163 to -153°C (Verwey, 1939). Due to non-stoichiometry or impurities this transition can be successively shifted towards lower temperatures or dis-

appears (Kakol and Honig, 1989; Özdemir et al., 1993; Moskowitz et al., 1998). During heating in argon atmosphere, a drop in susceptibility at about 584°C indicates the T_C of magnetite, confirming the low temperature interpretation. In the cooling run only slight to moderate irreversibility is observed. The χ - T curves of all other samples in this study are relatively similar. All samples show a Verwey transition with peak temperatures between -160 and -154°C indicating small variations in the degree of oxidation of magnetite (in terms of non-stoichiometry). The Curie temperatures are very consistent and range from 580 to 584°C . For some samples a Hopkinson peak just below T_C is observed, suggesting small grain sizes (Fig. 8a and c). During heating in argon atmosphere a more or less developed hump at about 120 – 380°C is observed in these samples.

According to χ - T curves, again the two groups of magnetic behavior can be distinguished (Fig. 8b and c).

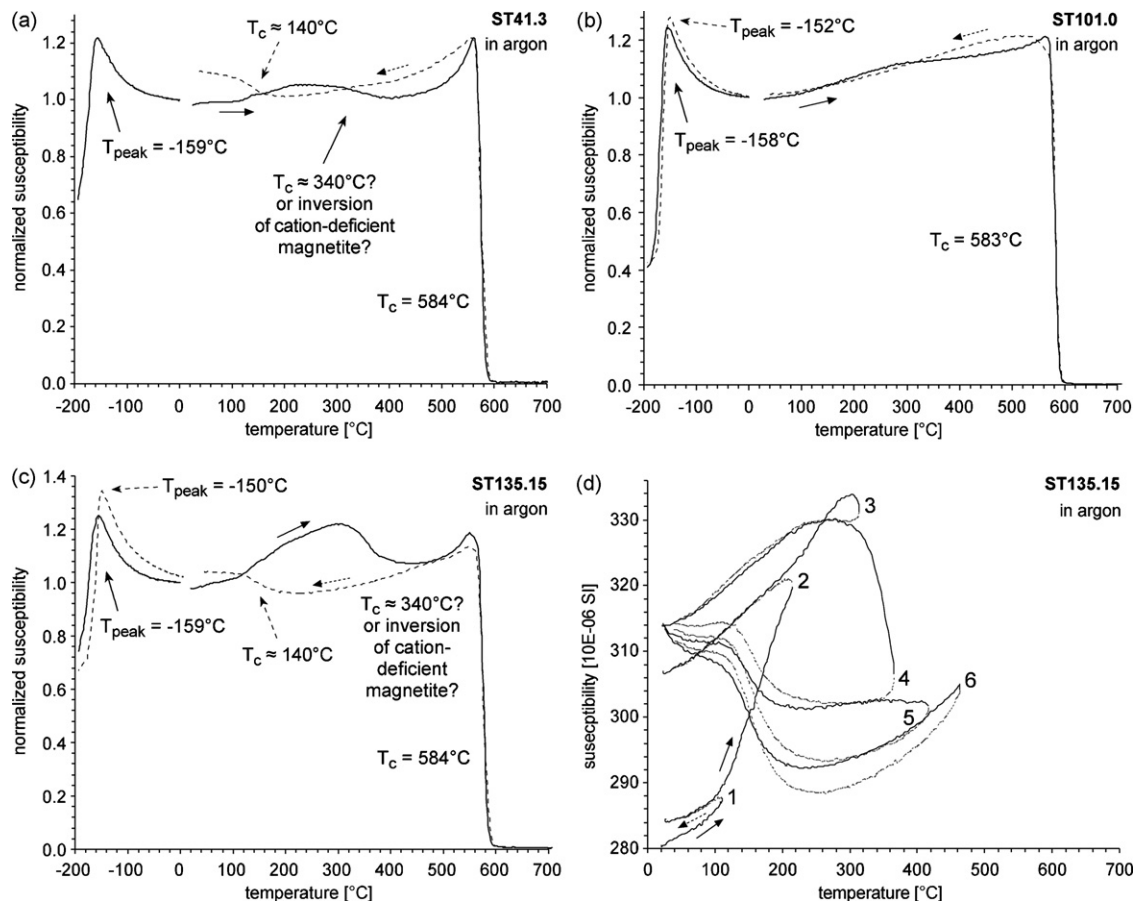


Fig. 8. Examples of temperature dependent susceptibility measurements done in argon (a–c); (d) stepwise heating in argon of ST135.15 to display the temperature intervals at which irreversibility occur (solid line: heating, dashed line: cooling (also indicated by arrows) and repeated low temperature measurement, respectively).

Group 1 (ST101.0) is characterized by a peak at the Verwey transition, one Curie temperature at 583 °C and a very good reversibility of the heating and cooling branch during measurement in an argon atmosphere. A second low temperature measurement shows a slightly higher Verwey transition temperature than the first low temperature measurement (Fig. 8b). Group 2 (ST135.15) also displays the peak at the Verwey transition but the measurement between room temperature and 700 °C shows a second magnetic phase in the heating run with a magnetic transition (or phase transition?) temperature at 340 °C. This phase is unstable during the heating experiment and in the cooling run a phase with a magnetic transition temperature at about 140 °C occurs instead. Instability of some magnetic phases during heating is reported in several studies (e.g. Keefer and Shive, 1980; O'Reilly, 1983) and the hump from our study can be most likely interpreted as a T_C or inversion of (titano)maghemite.

Another possible candidate to explain the unstable phase could be ilmenohematite with intermediate composition. But remanence experiments (see Fig. 7) exclude the presence of a higher coercive ferrimagnetic phase. Furthermore, electron microprobe analysis of ilmenohematite gave only Ti-rich compositions near ilmenite with T_N well below room temperature.

In order to better define the onset of irreversibility, stepwise heating experiments in argon atmosphere (Fig. 8d) were done. We first heated the sample to 100 °C and cooled it, then we heated the same sample to 200 °C and cooled it again. These heating–cooling cycles were repeated up to 700 °C (for clarity only the measurements up to 450 °C are displayed in Fig. 8d). According to this experiment the phase with the magnetic transition temperature at 140 °C appears first when the sample is heated up to 350 °C (measurement 4). This is clear evidence, that the breakdown of the phase with the T_C of about

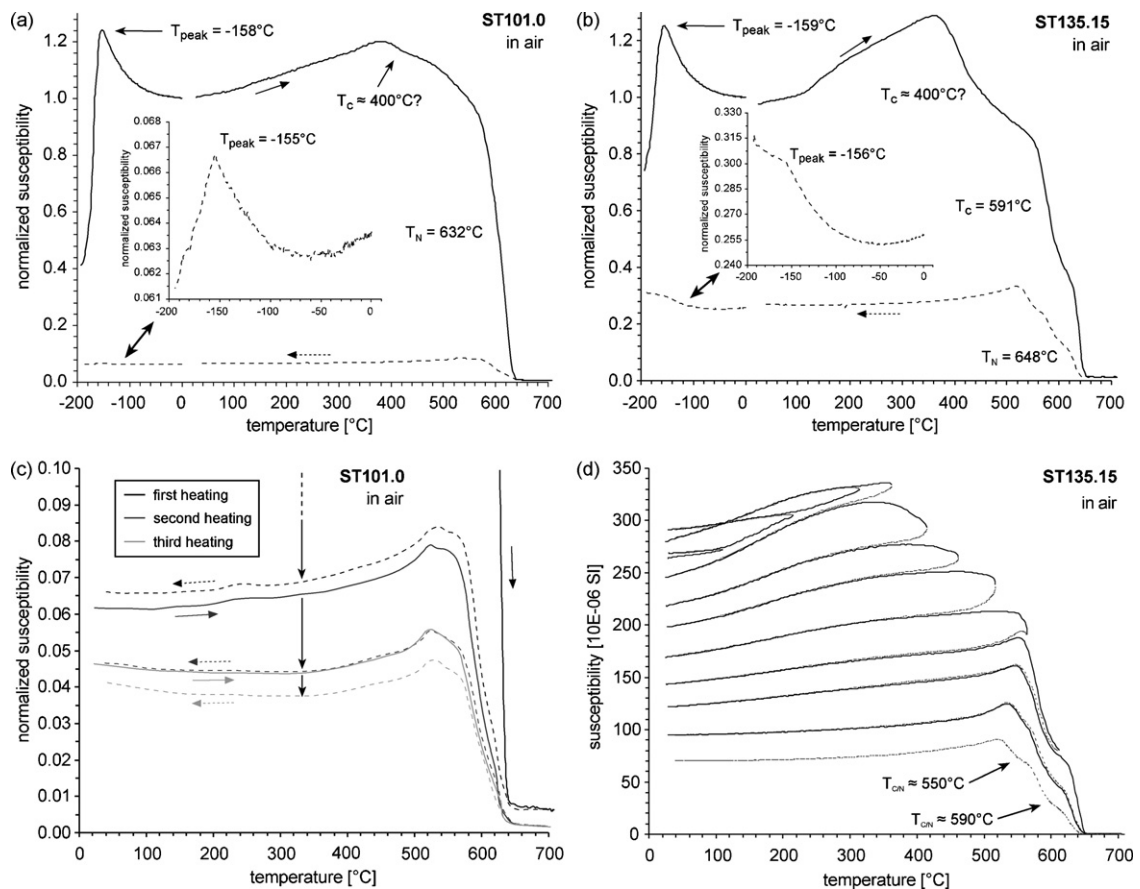


Fig. 9. Temperature dependent susceptibility for ST101.0 (a) and ST135.15 (b) done in air with subsequent re-measurement of the heated material (the inset shows the low temperature measurement with higher resolution); (c) multiple heating in air to 700 °C of ST101.0 showing the successive decrease in susceptibility which results in poor reversibility; (d) stepwise heating in air of ST135.15 to display the temperature intervals at which irreversibility starts (solid line: heating, dashed line: cooling (also indicated by arrows) and repeated low temperature measurement, respectively).

340 °C is directly related to the formation of the phase with the T_C at 140 °C. Furthermore, our experiment has shown, that this phase, once formed, is stable during heating. Curie temperatures at about 140 °C are reported for ferrihydroxides, e.g. goethite (αFeOOH) at 120 °C (Dunlop and Özdemir, 1997) or ferroxhyite (δFeOOH) at 177 °C (Murad, 1996). But ferrihydroxides are not stable during heating to 700 °C, e.g. goethite converts to hematite (Dunlop and Özdemir, 1997). Therefore, we assume that this hump is most likely related to an inversion of titanomaghemite to titanomagnetite of intermediate composition due to annealing and reduction reaction in argon atmosphere.

Stoichiometric synthetic and natural magnetite shows a very good reversibility of the heating and cooling curve in an argon atmosphere as well as in air flow (own unpublished data). Therefore, we measured our representative Stardalur basalts additionally in air flow (Fig. 9a and b) to better understand the irreversibility of our samples and its implication. During the measurement in an air flow, both samples show a more or less developed hump with T_C at about 400 °C, which is most likely attributed to titanomaghemite, that has been observed already in the argon measurement of ST135.15 (Fig. 8c). A second, very high $T_{C/N}$ at 632 and 648 °C, respectively, is probably related to an ilmenohematite with very low Ti content. This ilmenohematite is partly produced by the conversion of instable titanomaghemite during heating. Additionally, for ST135.15 a further T_C at 591 °C occurs, which is not seen in the χ - T curve of ST101.0. This third transition temperature is related to relics of the cation-deficient magnetite, which also converts to Ti-poor ilmenohematite due to oxidation during heating in air. This interpretation is in agreement with the strong irreversibility of the cooling run for both samples, which shows much lower susceptibilities. These low susceptibilities are in accordance with the formation of a mineral with much lower χ -values as, e.g. Ti-poor ilmenohematite. According to Hunt et al. (1995 and references therein) magnetic susceptibility of hematite is 20 times smaller than that of magnetite/maghemite. A very small contribution of magnetite/cation-deficient magnetite to the cooling curve is still verified by the second low temperature measurement, which displays only a very weakly developed Verwey transition (see inset with large magnification in Fig. 9a and b). These results indicate that Ti-poor ilmenohematite is produced during heating as a result of titanomaghemite conversion (see, e.g. Dunlop and Özdemir, 1997) and oxidation of cation-deficient magnetite, respectively.

Repeated heating to 700 °C in air atmosphere proved the stability of the once formed Ti-poor ilmenohematite

(Fig. 9c). While the Néel temperature does not change, the amplitude of magnetic susceptibility decreases due to progressive oxidation resulting in further irreversibility. Fig. 9d shows stepwise multiple heating experiments up to 700 °C (with increasing maximum temperature) to find the temperature at which the formation of ilmenohematite starts. The first three heating steps up to 300 °C reveal increasing susceptibilities similar to the single measurement up to 700 °C (Fig. 9b). This behavior is probably related to stress relaxation and/or unpinning of domain walls of the titanomaghemite with a T_C at about 400 °C during heating (Özdemir and Dunlop, 1997). Irreversibility with lower susceptibilities of the cooling branch starts after heating to 350 °C suggesting successive conversion of titanomaghemite to ilmenohematite as well as instability of cation-deficient magnetite. In the 550 °C step, only a slight increase in susceptibility during heating occurs, indicating that the phase with the T_C at about 400 °C is almost completely transformed. While increasing the maximum temperature, each step results in a similar degree of irreversibility. The occurrence of three phases with $T_{C/N}$ between about 550 and 640 °C appear first in the cooling run back from 650 °C. These phases are stable during further heating experiments. The third phase with $T_{C/N}$ of about 550 °C is only observed for ST135.15, while the phase with $T_{C/N}$ of about 590 °C is only weakly developed for ST101.0.

Our observations from χ - T curves suggest that the magnetic properties of the Stardalur basalts are mainly related to slightly cation-deficient magnetite and different amounts of titanomaghemite. This interpretation is corroborated from the heating and cooling behavior in argon atmosphere and air flow, and the lower Verwey transition temperature compared to stoichiometric magnetite during the first cooling run. In a second cooling run, the peak at the Verwey transition is shifted 6–9 °C to higher temperatures after heating in an argon atmosphere. The maximum transition temperature reported for pure stoichiometric single-crystal magnetite is -149 °C, whereas cation-deficiency or impurities depress the transition temperature down to -191 °C (e.g. Aragón et al., 1985a; Özdemir and Dunlop, 1998; Muxworthy and McClelland, 2000). Considering the findings of Aragón et al. (1985b) the shift of the Verwey transition before and after heating is equivalent to a lower degree in cation-deficiency (δ) by 0.002–0.003 ($\text{Fe}_{3(1-\delta)}\text{O}_4$). We assume that the annealing process during heating in argon heals cation defects and produces a more stoichiometric magnetite. This conversion from cation-deficient magnetite to more stoichiometric magnetite during heating has not been described in earlier studies.

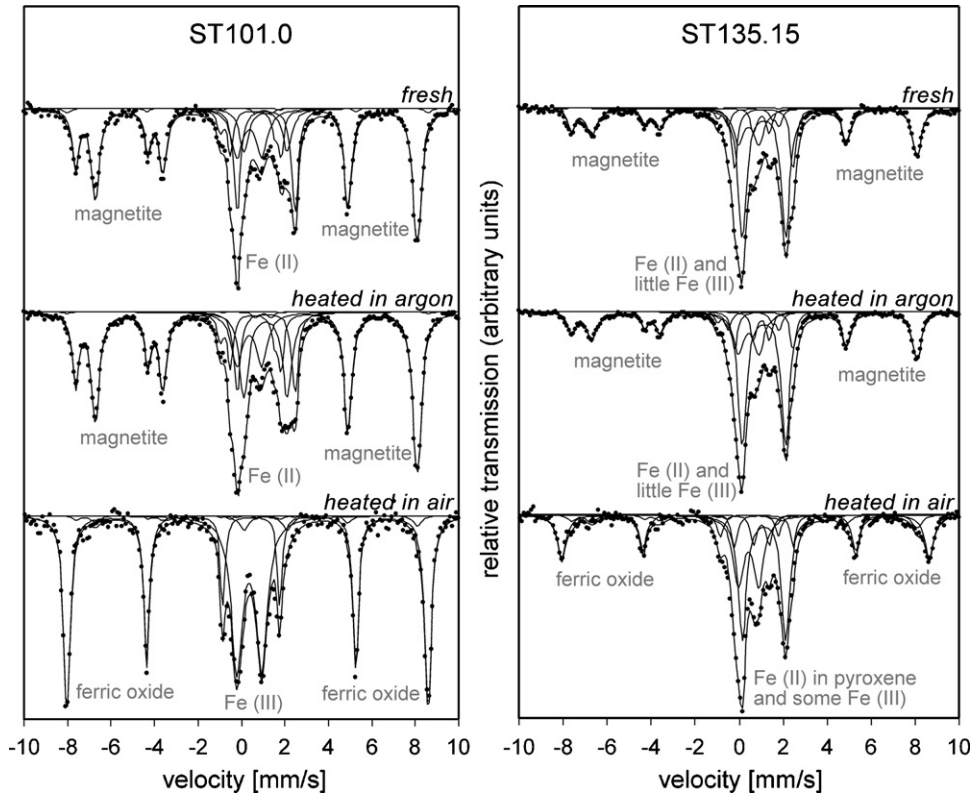


Fig. 10. Mössbauer spectra of fresh material and material used for temperature dependent susceptibility measurements in argon and air of ST101.0 and ST135.15.

3.5. Mössbauer spectroscopy

From the two representative samples ST101.0 and ST135.15 Mössbauer spectroscopy was performed in order to characterize the iron mineralogy and to resolve the changes taking place during heating in argon and air atmosphere. Fig. 10 shows Mössbauer spectra for the fresh and heated materials. The spectra of each sample were analyzed simultaneously, i.e. assuming the presence of the same components in varying amounts. The spectra were analyzed in terms of three sextets and four symmetric quadrupole split doublets.

The sextets were assigned to A and B line of magnetite constrained to have the empirical area ratio $B/A = 1.9$ and zero quadrupole shift ($2\varepsilon = \Delta E_Q = 0.0$ mm/s) and a ferric oxide. The internal area ratio of sextet lines were 3:2:1:1:2:3. The lines were assumed pair-wise alike (i.e. lines 1 and 6, 2 and 5, 3 and 4 having the same line-width (Γ), respectively). Due to overlap of the inner lines (3 and 4) with paramagnetic components, the constraint $\Gamma_{25} = (\Gamma_{16} + \Gamma_{34})/2$ was applied. The doublets were assigned to ilmenite, Fe(II) in pyroxene, unspecific Fe(III) and a Fe(II) having relatively high quadrupole splitting (results are listed in Table 2). The

hyperfine parameters of magnetite are found to be in good agreement with the assignment and the slightly reduced field from table values suggesting small level of impurities. The hyperfine field and the quadrupole shift of the ferric oxide denote that this component originates from hematite. The quadrupole splitting of the Fe(II) component is reduced in comparison with olivine, but is consistent with serpentine or a mixture of both. Small misfits in the spectra could suggest a small level of non-stoichiometry of magnetite or the presence of maghemite <3% of the spectral area of fresh samples. These results agree largely with Helgason et al. (1990), who found pure and homogeneous magnetite as the magnetically relevant mineral. But according to the $\chi-T$ curves presented above (Fig. 8 and 9) it is likely, especially in respect to the shift in Verwey transition temperature and the strong irreversibility, that the magnetite is slightly non-stoichiometric. Indeed, the Mössbauer spectrum can be interpreted in terms of non-stoichiometry up to $\delta \approx 0.01$, which corresponds to a shift of the Verwey transition by 30 °C, which is not the case. The $\chi-T$ measurements therefore seem to be more sensitive to non-stoichiometry than Mössbauer spectroscopy.

Table 2
Hyperfine parameters obtained from simultaneous analysis of the spectra of ST101.0 and ST135.15 samples

ST101.0	Magnetite_A	Magnetite_B	Ferric oxide	Fe(II)	Fe(II) pyroxene	Fe(III)	Ilmenite
B_{hf} (T)	48.93(5)	45.69(4)	51.45(4)				
δ (mm/s)	0.288(6)	0.666(4)	0.375(5)	1.146(6)	1.12(1)	0.37(2)	1.02(2)
ΔE_{Q} (mm/s)	0	0	-0.17(1)	2.66(2)	1.99(4)	1.14(2)	0.7(2)
Γ_{16} (mm/s)	0.36(2)	0.45(2)	0.36(2)	0.36(3)	0.51(4)	0.61(3)	0.3(3)
Γ_{34} (mm/s)	0.34(4)	0.30(2)	0.26(2)				
A_fresh (%)		56(3)	1.6(9)	17(2)	10(2)	13(2)	0.8(9)
A_Ar (%)		58(2)	0.5(7)	11(2)	16(2)	12.5(9)	0.8(8)
A_air (%)		3(2)	55(3)	0.3(10)	3(2)	36(3)	0.3(10)
ST135.15	Magnetite_A	Magnetite_B	Ferric oxide	Fe(II)	Fe(II) pyroxene	Fe(III)	Ilmenite
B_{hf} (T)	48.8(1)	45.61(8)	51.7(2)				
δ (mm/s)	0.27(2)	0.67(1)	0.38(2)	1.13(1)	1.139(4)	0.44(1)	1.03(1)
ΔE_{Q} (mm/s)	0	0	-0.18(3)	2.66(1)	1.969(3)	0.93(3)	0.71(3)
Γ_{16} (mm/s)	0.37(3)	0.54(4)	0.47(2)	0.32(2)	0.451(5)	0.57(4)	0.32(4)
Γ_{34} (mm/s)	0.28(6)	0.30(3)	0.32(2)				
A_fresh (%)		30(2)	0(2)	12.8(5)	38.0(9)	13(1)	5.1(3)
A_Ar (%)		31(2)	0(2)	8.1(3)	39.6(9)	15.2(4)	5.9(8)
A_air (%)		7(2)	25(2)	6.0(8)	32(2)	22(2)	5.5(2)

The numbers in the parentheses represent 1σ error in the last digit. Quadrupole shift of sextet components is given as 2ε

Generally, the difference in Mössbauer spectra between fresh ST101.0 and ST135.15 are at least two-fold: (1) spectra of ST101.0 lack an ilmenite signal, which is consistent with microscopic observations (only very fine-grained exsolved titanomagnetite, according to electron microprobe analysis less than 0.54 wt.% TiO_2), (2) a significantly larger contribution of magnetite to the Mössbauer spectra of ST101.0 as reflected by the higher area percentage (56 comparing to 30) resulting in higher NRM intensity and χ . The spectra of material heated in argon atmosphere show almost no change in comparison to the fresh material, in agreement with the χ - T curves of Fig. 8b and c. But significant differences can be observed for the samples heated in air atmosphere. For ST101.0 a large contribution of ferric oxide (hematite with perhaps a small contribution of maghemite) is found, to which the magnetite has completely altered, whereas a small amount of magnetite (7%) is remaining for ST135.15. But also for ST135.15, almost all of the (cation-deficient) magnetite is transformed to ferric oxide (hematite) during measurement in air atmosphere. The Fe(II) component bonded to silicates like, e.g. chlorite is higher for ST101.0. Furthermore, almost the entire Fe(II) is lost during heating in air, whereas for ST135.15 Fe(II) is still present. This relation suggests a higher amount of thermally unstable minerals like, e.g. chlorite for ST101.0 and supports the hypothesis of stronger alteration affecting ST101.0. This excellent correlation between χ - T curves and Mössbauer spectra corroborates that the χ - T measurements can be used as a reliable

method for the identification of ferromagnetic iron mineralogy.

4. Discussion

The strong magnetic anomaly at the Stardalur volcanic complex, situated about 20 km NE of Reykjavik, is caused by an extraordinary strong remanent magnetization of up to 121 A/m related to a high magnetite content. According to different previous studies, following factors seem to account for the unusually high magnetization of these basalts: (1) small grain size, (2) high temperature oxidized titanomagnetite, resulting in almost pure magnetite, (3) symplectic magnetite from oxidized olivine and (4) higher (local) paleomagnetic field intensity (Fridleifsson and Kristjansson, 1972; Helgason et al., 1990; Gunnlaugsson et al., 2003, 2006). However, these features are not unique for the Stardalur basalts and therefore we will revisit different mechanisms controlling abundance, composition and grain size in relation to geologic processes.

According to our rock magnetic and magneto-mineralogical investigations the magnetically relevant mineral in these rocks is mainly cation-deficient magnetite. From microscopic observations and the comparison with, e.g. Hawaiian basalts (Kontny et al., 2003; Vahle, 2005) we can conclude that multiple processes, related to the geodynamic setting, the emplacement and the cooling history of the basalts, affected the texture and composition of the originally homogeneous titanomag-

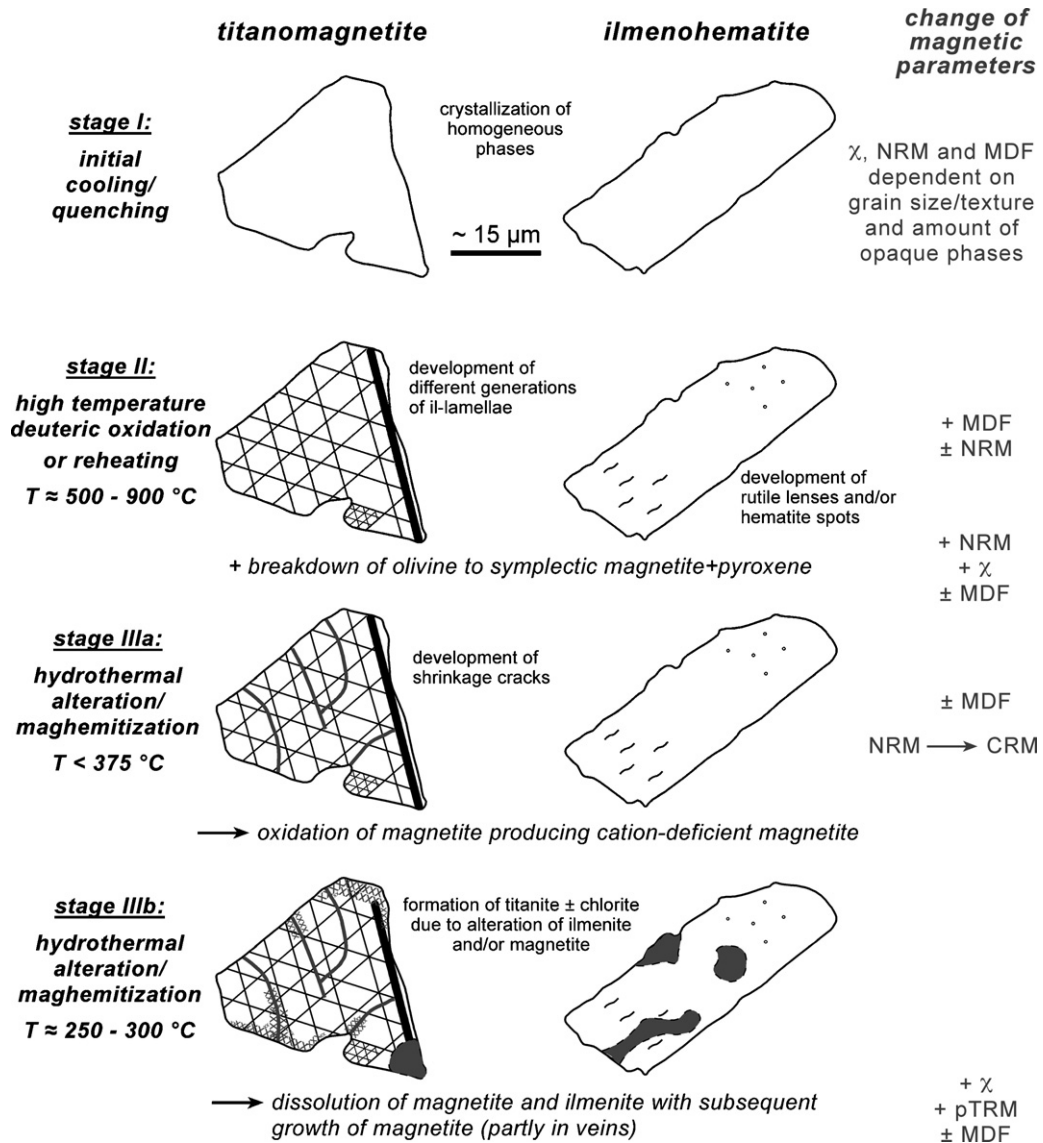


Fig. 11. Sketch showing the development of titanomagnetite and ilmenohematite textures from initial cooling/quenching to the latest stage of alteration; additionally, the change in strength of the relevant magnetic parameters is given (further description see text).

magnetite (stage I in Fig. 11) resulting in extraordinarily high NRM intensity and magnetic susceptibility. These processes are discussed in the following section.

4.1. Magma composition and cooling history

During initial cooling and quenching of the lava, the rock acquires a TRM, which depends on the amount and grain size of titanomagnetite. Amount and grain size in turn depend on the lava composition, degree of undercooling and cooling rate (\pm oxygen fugacity) during lava emplacement. Gee and Kent (1997) derived a relationship between FeO_{tot} as an indica-

tor of magma fractionation of submarine glass and NRM ($\text{NRM [A/m]} = -25.8 + 4.44 \times \% \text{FeO}_{\text{tot}}$) for axial lavas from the southern East Pacific Rise. Taking a range of 8.5–14.3 wt.% FeO_{tot} for Icelandic basalts from the Reykjanes peninsula (picritic to tholeiitic basalts described in Jakobsson et al., 1978) NRM intensities of 12–38 A/m could be acquired according to this relationship. This NRM intensity range fits nicely to own unpublished data of surface basaltic rocks from SW-Reykjanes peninsula: 4–32 A/m (reduced to 90 % of the data set to exclude extreme values). On the other side, a correlation of geochemical data (Rhodes and Vollinger, 2004; Stolper et al., 2004) and NRM inten-

sities (Vahle, 2005) of subaerial and submarine basalts from the Hawaiian Scientific Drilling Project (HSDP-2) gave no reasonable results. In this geodynamic setting the measured NRM intensities (<1–13 A/m, 90% of the data) are much lower than the calculated values on the base of Gee and Kent's (1997) equation (18–32 A/m). However, Steinthorsson and Sigvaldason (1971) have found for Stardalur basalts a rather high Fe-content of ~12 wt.%. Using this value in Gee and Kent's (1997) equation one gets 43 A/m, which is far below the average of 63 A/m. These observations indicate, that besides total Fe-content of the magma, other factors must also control the remanence intensity.

More important for the resulting magnetic mineral assemblage than the total Fe-content is the Ti/(Ti + Fe) ratio and the oxygen fugacity of the melt. High Ti/(Ti + Fe) ratios at the same oxygen fugacity favor the formation of Ti-rich phases like ilmenohematite, while decreasing Ti/(Ti + Fe) ratios enable a higher amount of titanomagnetite at a fixed oxygen fugacity. This relationship was shown in experimental studies in the Fe–Ti–O system (see, e.g. Fig. 2 in Lattard et al., 2006) and is especially true for compositions above the NNO buffer. The generally high amount of magnetic titanomagnetite in the Stardalur basalt seems to be in agreement with relatively oxidized conditions of the basalt melt (above the NNO buffer) and low Ti/(Ti + Fe) ratios. Except for one single analysis of a sample from 60 m depth, no geochemical data are available for the Stardalur basalts up to now. But analyses from surface rocks of the Reykjanes peninsula (SW-Iceland) by Jakobsson et al. (1978) revealed compositions lower in titanium (total iron is similar, resulting in lower Ti/(Ti + Fe) ratios) in comparison with data from, e.g. HSDP-2 basalts (Rhodes and Vollinger, 2004; Stolper et al., 2004). The single Stardalur analysis has slightly higher total iron and titanium resulting in Ti/(Ti + Fe) ratios intermediate between Reykjanes and Hawaii. Both, the Reykjanes and Hawaiian basalts show in part similar concentrations of Fe–Ti oxides, but the Icelandic rocks exhibit mostly significantly higher NRM intensity and magnetic susceptibility. This feature is related to the lower ilmenohematite contents of the Icelandic basalts, reflecting a magma composition with low Ti/(Ti + Fe) ratio, resulting in higher titanomagnetite abundance relative to ilmenohematite and therefore higher NRM intensity and χ .

Investigations on the remanence properties of synthetic Fe-rich basalts (18.9% FeO_{tot}) from Brachfeld and Hammer (2006) have shown that the acquisition of thermoremanent magnetization is linked to the oxygen fugacity of the melt and the resulting magnetic

mineral assemblage. Samples synthesized at the iron-wüstite (IW) buffer have a very low concentration of remanence-carrying grains, samples synthesized at the quartz-fayalite-magnetite (QFM) and nickel-nickel oxide (NNO) buffers contain a slightly higher amount, and samples synthesized at the manganese oxide (MNO) buffer show the highest concentration of magnetic grains, which are up to 100 μm in diameter. The QFM, NNO and MNO samples acquired TRMs up to 40 A/m in a 10 μT field and even 200 A/m in a 50 μT field, with little or no dependence on cooling rate. However, such high values have rarely been observed in terrestrial basalts except zero-age pillow basalts from the East Pacific Rise (Carlut and Kent, 2002) and some basalt occurrences on Iceland (e.g. Gunnlaugsson et al., 2006; this study). Moreover, Carlut and Kent (2002) found strong internal NRM variations on a millimeter scale, whereas the remanence increases sharply in the first centimeter from the marginal part to the pillow interior. This pattern is directly related to a different cooling history in the specific parts of the pillow. In the marginal parts almost no crystals appear due to solidification in less than a few seconds (Griffiths and Fink, 1992), whereas the inner part cooled slower (~250 °C/h) leading to rapid formation of magnetic minerals of up to ~40 μm in size (Zhou et al., 2000). Therefore, both oxygen fugacity and cooling rate must be considered as major parameters affecting the magnetic properties.

For the Stardalur basalts two groups have been defined based on the rock magnetic and magnetomineralogical properties. The texture and grain sizes of group 1 (ST101.0; dendritic to cruciform titanomagnetite, 5–20 μm in size) reflect faster cooling in comparison to the group 2 (ST135.15; bimodal spectrum with dendritic to euhedral grains of <10–80 μm size). In samples of group 2 a dense network of ilmenite-lamellae points to high temperature deuteric oxidation during slower cooling. The difference in NRM intensity and χ of these two groups is mainly related to the opaque mineral content and its texture, which depends strongly on cooling history as their primary composition should be the same. After their emplacement the Stardalur basalts suffered significant oxidation and alteration. Therefore, we discuss more closely the processes during and after cooling as further possible mechanisms for the enhancement of the already high magnetization.

4.2. High temperature deuteric oxidation

Oxide textures of the Stardalur samples imply high temperature deuteric oxidation during cooling of the lava. This oxidation is typical for subaerial basalts

and is responsible for a significant grain size reduction due to multiple sets of Ti-rich ilmenohematite exsolution-lamellae (e.g. Fig. 4b) within the originally homogeneous titanomagnetite (see stage II in Fig. 11). This oxyexsolution causes a distinct increase of coercivity but not NRM intensity as our studies on basalt drill cores from the HSDP-2 have shown (Kontny et al., 2003; Vahle, 2005). Basalts from the subaerial section of the HSDP-2 drill core with homogeneous titanomagnetite show a T_C of 100 °C ($X_{\text{usp}} \approx 0.70$), while for samples with exsolved titanomagnetite a T_C at 520 °C ($X_{\text{usp}} \approx 0.10$) is observed. Both samples have comparable NRM intensities ranging between 5 and 6 A/m. Therefore, high temperature deuteric oxidation seems not to be a significant mechanism leading to an increase in NRM intensity but it enhances remanence stability (MDF of 14 mT and less for samples with homogeneous titanomagnetite and up to 45 mT for exsolved ones).

Additionally to the oxidation of Fe–Ti oxides, silicate minerals are altered during this second stage (Fig. 11) forming magnetite, which acquires a stable (T)CRM. Symplectic magnetite (+ pyroxene) is produced by the breakdown of olivine through high temperature deuteric oxidation or reheating (Section 3.1 and Figs. 4a and 11). This magnetite formation leads to an increase in NRM intensity and χ . The reheating could be induced by later dike intrusions or burial by a new lava flow. Kristjansson (1985) studied the magnetic and thermal effect of dike intrusions (average width of 4 m) into relatively fresh subaerial lava piles in Iceland. The affected area reached less than 0.5 m away from the contact into the lava flows, whereas changes in remanence intensity cannot be clearly resolved due to primary variations. But a change in remanence direction points to a later overprint. On the contrary, Bleil et al. (1982) found abundant secondary magnetite in altered subaerial basalts drilled by the Iceland Research Drilling Project (IRDP) in E-Iceland. This secondary magnetite, which is interpreted to increase NRM intensity and which changed magnetic polarity, occurs in zones of dense dike intrusions, providing heat for the remagnetization of the lava flows. Furthermore, Hall (1985) reported on samples from the same drilling an increase of χ and magnetization (induced and remanent) towards the dike contacts, which is related to the growth of secondary magnetite leading to a partial to complete remagnetization of the lava flows. According to the lithological descriptions of the Stardalur core, no intrusions have been found, and the discharge of hydrothermal fluids provides not enough heat for the development of symplectic magnetite (>810 °C, Haggerty and Baker, 1967), leaving reheating by burial beneath younger lava flows as the

only other option. Possible reheating is reflected in the recrystallized glass shards of the hyaloclastite sample ST41.3 and the growth of abundant magnetite lining the glass shards. This leads to unusually high NRM intensity and χ (Table 1) of hyaloclastite, which is usually characterized by low values due to strong quenching in water, where only few, small crystals can develop. Therefore, a rather less magnetic behavior (lower magnetization and susceptibility) is expected for those kinds of rocks (see, e.g. Kontny et al., 2003; Vahle, 2005).

Indeed, Gunnlaugsson et al. (2006) attribute the high magnetization (40 A/m) of some of their Sudurdalur samples (E-Iceland) to the development of symplectic magnetite (by alteration of olivine). Samples with relatively fresh olivine show only 4 A/m, pointing to a strong increase of NRM intensity due to formation of symplectic magnetite. Although, in our Stardalur samples this mechanism seems to be of less importance comparing to the studies of Gunnlaugsson et al. (2006), we found some indications for symplectic magnetite, which locally increases NRM intensity to some extent, especially in regard to the high temperature of remanence acquisition near and above T_C resulting in a TRM (see below for explanation). Therefore, this mechanism seems to be one important factor contributing to the high magnetization values of the Stardalur basalts.

4.3. Hydrothermal alteration

A significant feature of titanomagnetite in the Stardalur samples is the shrinkage cracks (e.g. Figs. 4c, 5c and d), which are a microscopic sign for maghemitization (Petersen and Vali, 1987). Generally, maghemitization is described as a low temperature (<200–250 °C) process occurring mainly at the crystal surface or along cracks promoted by an aqueous environment (e.g. Dunlop and Özdemir, 1997). Depending on subaerial or aqueous conditions, the mechanism is oxidation of Fe^{2+} to Fe^{3+} at a crystal surface and diffusion of Fe^{2+} from the crystal interior to a free surface, where the ion is removed and dissolved in water. Oxidation is therefore a slow process, partly controlled by diffusion rates of Fe^{2+} and the distance to the surface. As a result, the oxidized titanomagnetite gets enriched in Fe^{3+} . Due to removal of Fe^{2+} charge balancing vacancies are created leading to the generation and increase of internal stresses in the crystal lattice until it breaks.

Curie temperatures of maghemite are reported between 470 and 695 °C (Dunlop and Özdemir, 1997, and references therein), but it can seldom be measured because it usually inverts to magnetite or hematite between 250 and >750 °C. On the contrary, e.g. Helgason

et al. (1992) found stable maghemite in olivine basalts from Iceland using Mössbauer spectroscopy. At 600 °C maghemite is stable in an oxidizing environment for several hours, little maghemite is present after heating for 2 h in an inactive atmosphere, while the maghemite converts to magnetite already after 30 min under reducing conditions (see also Gunnlaugsson et al., 2002). The χ - T measurements in argon and air of all other samples point to cation-deficient magnetite converting to (stoichiometric) magnetite and Ti-poor ilmenohematite, respectively (Figs. 8a–c and 9a and b). The irreversibility, observed during our measurements, is probably related to cation-deficient magnetite, which is less stable during heating, in comparison to a rather stable behavior of fully oxidized maghemite found by, e.g. Helgason et al. (1992) and Gunnlaugsson et al. (2002).

Maghemite or titanomaghemite has also been reported, e.g. by Steinthorsson et al. (1992) and Gunnlaugsson et al. (2002) for different Icelandic basalts. The first group of authors suggests the onset of maghemitization taking place subsequent to hydrothermal alteration during burial and reheating of the lava flows at wet conditions. Gunnlaugsson et al. (2002) observed an increase in titanomaghemite content after heating the samples (mixture of titanomagnetite and titanomaghemite) to 500–600 °C at oxidizing conditions. During this experiment, titanomagnetite gets depleted in Ti due to exsolution processes. Additionally, hematite forms when heated to \sim 700 °C. In case of the Stardalur basalts the instability of titanomaghemite and cation-deficient magnetite starts at \sim 350 and \sim 400 °C, when heated in argon and air atmosphere, respectively (Figs. 8d and 9d). Therefore, their maghemitization must have occurred mainly below \sim 375 °C on a retrograde path during hydrothermal alteration. Hydrothermal activity is indicated by the presence of zeolites, montmorillonite and chlorite occurring in the groundmass and in vesicles (stage IIIa in Fig. 11). Our thermomagnetic measurements suggest, that no cation-deficient (titano)magnetite should have survived in the basalt, if the rocks would have been reheated to $>$ 400 °C after maghemitization.

Maghemitization of ocean basalts is suggested to cause a decrease of NRM intensity (e.g. Matzka et al., 2003), which is explained by the lower saturation magnetization of titanomaghemite compared to titanomagnetite (e.g. magnetite: 480 kA/m, maghemite: 380 kA/m, Dunlop and Özdemir, 1997). But the development of shrinkage cracks divides the grain into smaller pieces and possibly leads to an increase or at least no change in NRM intensity as far as no magnetostatic interactions occur. Studies of Helgason et

al. (1992) and Gunnlaugsson et al. (2002) suggested titanomaghemite as the stable carrier of NRM intensity in Icelandic basalts. Therefore, oxidation of titanomagnetite to titanomaghemite must not necessarily lead to a reduced NRM intensity. For samples from the HSDP-2 even a slight increase of NRM intensity with depth (and age) is observed, despite the occurrence of low temperature oxidized titanomagnetite (Vahle, 2005). Comparing the different temperature stability of ST101.0 and ST135.15 (Figs. 6b and c, 9a and b) one may expect a stronger degree of maghemitization (and overall alteration) for ST101.0 due to stronger irreversibility during heating in air (see also significantly lower χ after thermal demagnetization to 700 °C). At least three explanations are conceivable up to now for this difference: (1) ST101.0 exhibits a stronger degree of cation-deficiency resulting in stronger thermal instability (due to small grain sizes diffusion has almost totally affected the grains), (2) ST135.15 is less sensitive to maghemitization because some parts of the oxidized titanomagnetite grains resist maghemitization due to the large grain size (slower diffusion, oxidation not uniform but varies with grain diameter), and (3) ST101.0 contains more magnetite derived from oxidation of olivine (this magnetite has less thermal stability than magnetite derived from exsolution of titanomagnetite). If this is true, the stronger “maghemitized” (altered) sample (ST101.0) shows much higher NRM intensity and χ , which opposes studies of, e.g. Matzka et al. (2003). Although these higher values are mostly related to other factors like grain size and concentration of magnetic minerals, this relation implies, that in case of the Stardalur basalts maghemitization during stage IIIa hydrothermal alteration did not lead to a significant lowering of NRM intensity.

The maghemitization at stage IIIa and the associated shrinkage cracks in the oxidized titanomagnetite crystals served as pathways for hydrothermal fluids, which altered titanomagnetite as well as ilmenohematite along the cracks and at the margins (Fig. 4c) by dissolution. This alteration leads to the formation of titanite \pm chlorite (stage IIIb in Fig. 11), whereas the dissolution and replacement of ilmenite-lamellae in titanomagnetite created “ghost” textures (Fig. 4b). According to Ade-Hall et al. (1971) a minimum temperature of 250 °C is necessary for the replacement of ilmenite by titanite. Above 300 °C polycrystalline Ti-hematite occurs pseudomorph after titanomagnetite. As we have rarely observed hematite but titanite in various amounts, the temperature range of stage IIIb hydrothermal alteration was likely between 250 and 300 °C.

The dissolution of ilmenohematite (and titanomagnetite) during stage IIIb hydrothermal alteration probably supplied material for the growth of secondary magnetite (Fig. 4d–f), which could also contribute to higher NRM. Hall (1985) found an increasing amount of secondary magnetite partly produced during hydrothermal alteration in the lower section of the IRDP especially where primary magnetite has been dissolved. The secondary magnetite contributes to an increase of χ (depending on the ratio of dissolved/newly grown magnetite). Because of the good correlation between NRM and χ (Fig. 3) the formation of secondary magnetite is assumed to increase also NRM intensity, although this increase is presumably small. The intensity of a thermochemical remanence (CRM) acquired during crystal growth at temperatures well below T_C by this secondary magnetite is significantly lower than that of an initial TRM acquired during cooling from or just below T_C (e.g. Haigh, 1958; Kobayashi, 1959). Draeger et al. (2006) found for samples from a Quaternary basaltic dike (S-France) with single-domain titanomagnetite only half the remanence intensity acquired at 400 °C compared to a TRM. Remanence intensity could even be reduced due to intensive replacement of primary titanomagnetite grains. The different extent of increase in NRM intensity and χ is probably reflected in the relatively low values of Q -factor (5–32). In sight of the high NRM intensities of 18–121 A/m one would expect also high values for the Q -factor, especially when compared to rather fresh, young (<20 ka) surface samples from the Reykjanes peninsula with NRM intensity range between 4 and 32 A/m and Q -factors between 20 and 105 (90% of the data set, unpublished data). Therefore, it is likely that the growth of these secondary magnetite grains at intermediate to low temperatures (300–250 °C) leads to a significant increase in χ (and higher induced magnetization) but only slightly higher NRM. Due to the poor reversibility of χ - T curves in air (Fig. 9) it is likely, that this secondary magnetite also is slightly non-stoichiometric.

4.4. Paleomagnetic field intensity

Although paleointensity investigations are beyond the scope of our study, the intensity of the paleomagnetic field is one crucial factor for the intensity of NRM. Therefore, the influence of paleointensity on the NRM of the Stardalur basalts is discussed below.

From paleointensity studies it is concluded that the strength of the Earth magnetic field fluctuates over the Earth history (e.g. Gee et al., 1996; Wang et al., 2005). Wang et al. (2005) found an increase of NRM

intensity of Cretaceous Atlantic and Pacific MORB with increasing age following a depression at 10–30 Ma aged rocks. While the decrease of NRM intensities of maghemitized ocean basalts (e.g. Matzka et al., 2003) is explained by the lower saturation magnetization of titanomaghemite compared to titanomagnetite, Wang et al. (2005) excluded by a statistical approach compositional, petrologic, rock magnetic, or paleomagnetic patterns for the Cretaceous increase in NRM intensity. They suggested that the geomagnetic field intensity must have been significantly higher during the Cretaceous than during the Oligocene and Miocene.

Fridleifsson and Kristjansson (1972) suggested a higher field intensity of $93 \pm 6 \mu\text{T}$ for the Stardalur rocks, which is almost twice the current value for SW-Iceland. This is partly supported by Carmichael (1970) and Ade-Hall et al. (1972) who derived 64–120 μT on dredged Quaternary ocean basalts from 45°N, whereas Smith (1967) found only $34 \pm 3 \mu\text{T}$ for the upper Cenozoic. The thermal instability of the magnetic relevant phases in the Stardalur rocks hampers reliable paleointensity studies. TRM experiments in different laboratory fields from 15 to 145 μT applied on pillow basalts of the East Pacific Rise (Carlut and Kent, 2002) revealed an almost perfect linear relationship between TRM intensity and field amplitude. The NRM intensity of the Stardalur basalts could therefore be twice as high if they had cooled in a paleomagnetic field that had an intensity that was twice that of today.

In fact, Meynadier et al. (1995) suggested, that the geomagnetic field occasionally becomes quite strong (1.5–2 times the average), for instance when recovering after a reversal. The Stardalur basalts are estimated to be extruded during Olduvai Subchron based on two K–Ar datings of nearby rhyolites at the Stardalur caldera (Kristjansson et al., 1980). The Olduvai Subchron (1.95–1.77 Ma, Cande and Kent, 1995) is a normal polarity event during Matuyama Chron (negative polarity). Maybe, during this short time interval between polarity transitions the Earth magnetic field has been stronger. However, this increase in paleointensity during Olduvai Subchron has not been confirmed so far. In contrast, relative paleointensity studies on ODP-sediment cores from different localities (equatorial Pacific and Iceland basin 450 km south off Iceland) revealed almost no change for the Olduvai Subchron compared with earlier and later times (Meynadier et al., 1995; Channell et al., 2002; Yamazaki and Oda, 2005). A reasonable cause of higher field intensity is a local increase due to strongly magnetic underlying rocks, as already suggested by Fridleifsson and Kristjansson (1972). However, such an explanation remains vague.

5. Conclusions

The strong magnetic anomaly of the Stardalur volcanic complex in Iceland is caused by an extraordinary high remanent magnetization of up to 121 A/m. Although we still cannot present an unequivocal explanation for these extraordinary high values, our study suggests that high NRM is due to a high primary titanomagnetite content formed from a basaltic melt with high oxygen fugacity and low Ti/(Ti + Fe) ratio, related to the geodynamic setting on Iceland. Additional to magma composition and cooling history, multiple processes affected the texture and composition of the originally homogeneous titanomagnetite resulting in a further increase in NRM intensity and magnetic susceptibility.

According to our results, originally homogeneous titanomagnetite and ilmenohematite suffered subsequent high temperature deuteric oxidation and/or oxidation by later reheating from younger lava flows producing exsolution textures and symplectic magnetite. Due to the high temperatures of $\sim 500\text{--}900\text{ }^\circ\text{C}$ (stage II), especially the symplectic magnetite can acquire a high and stable TRM (due to the small grain sizes) increasing the NRM. Our own data and Gunnlaugsson et al. (2003) showed an unusually large proportion of iron located in magnetite (up to 56% of the area of the Mössbauer spectra, 5–10% is more usual), which is in accordance with the alteration of Fe-bearing silicates (predominantly olivine) at high temperatures with subsequent formation of magnetite, leading to an increase in NRM intensity and χ . The NRM (17.7 A/m) of the hyaloclastite sample at the top of the strongly magnetic basalt lava flows may give an approximation of this contribution to NRM.

During the first stage of hydrothermal alteration (stage IIIa, $T < 375\text{ }^\circ\text{C}$) cation-deficient (titano)magnetite is produced. This early hydrothermal stage seems not to be crucial for the NRM intensity of the Stardalur basalts (it either seems to decrease nor increase NRM significantly), but during maghemitization shrinkage cracks developed, which served as pathways for later stage hydrothermal fluids (stage IIIb, $T \approx 250\text{--}300\text{ }^\circ\text{C}$). These fluids partly dissolved the primary Fe–Ti oxides, leading to the formation of titanite and secondary magnetite (with further subsequent maghemitization), which is assumed to carry only a low remanence, whereas magnetic susceptibility increases significantly contributing to the induced magnetization.

Although the newly formed magnetite during this hydrothermal stage is not very important for the NRM intensity, we assume that hydrothermal alteration is the key factor for the formation of cation-deficient magnetite

from the already existing magnetic minerals. Cation-deficient magnetite is found to be the main carrier of the magnetic properties of the Stardalur basalts and for the first time, it is suggested to be the magnetically relevant mineral, responsible for the strong magnetic anomaly at Stardalur. Furthermore, for the first time the conversion from cation-deficient to more stoichiometric magnetite during laboratory heating has been observed. During this maghemitization the NRM intensity seems to be unchanged. The results of this study can be helpful in explaining other strong magnetic anomalies in basaltic environment on Earth and Mars.

Acknowledgements

First we want to thank our Icelandic colleagues from the Iceland GeoSurvey ISOR (G.O. Fridleifsson, A. Gudmundsson, A. Blischke, B. Gautason, H. Franzson) and from the Technical University of Iceland (H. Audunsson) for their excellent support and information exchange during our stay at Iceland in July 2005. Ann Hirt is acknowledged for her help and comments concerning the IRM and thermal demagnetization measurements at ETH, Zurich. Thanks to R. Harrison and R. Van der Voo for helpful reviews. The German Research Foundation is acknowledged for funding this work (No. KO1514/3).

References

- Acuña, M.H., Connerney, J.E.P., Ness, N.F., Lin, R.P., Michell, D., Carlson, C.W., McFadden, J., Anderson, K.A., Reme, H., Mazelle, C., Vignes, D., Wasilewski, P., Cloutier, P., 1999. Global distribution of crustal magnetization discovered by the Mars Global Surveyor MAG/ER experiment. *Science* 284, 5415–5427.
- Ade-Hall, J.M., Palmer, H.C., Hubbard, T.P., 1971. The magnetic and opaque petrological response of basalts to regional hydrothermal alteration. *Geophys. J. R. Astronom. Soc.* 24, 137–174.
- Ade-Hall, J.M., Ryall, P.J.C., Gerstein, R.E., 1972. Magnetic results from basalt drill cores from the M.A.R. median valley at 45°N . *Eos Trans.* 53, 955.
- Aragón, R., Buttrey, D.J., Shepard, J.P., Honig, J.M., 1985a. Influence of nonstoichiometry on the Verwey transition. *Phys. Rev. B* 31, 430–436.
- Aragón, R., Shepard, J.P., Koenitzer, J.W., Buttrey, D.J., Rasmussen, R.J., Honig, J.M., 1985b. Influence of nonstoichiometry on the Verwey transition in $\text{Fe}_{3(1-\delta)}\text{O}_4$. *J. Appl. Phys.* 57, 3221–3222.
- Baker, I., Haggerty, S.E., 1967. The alteration of olivine in basaltic and associated lavas. Part II. Intermediate and low temperature alteration. *Contrib. Mineral. Petrol.* 16, 258–273.
- Bleil, U., Hall, J.M., Johnson, H.P., Levi, S., Schönharting, G., 1982. The natural magnetization of a 3-kilometer section of Icelandic crust. *J. Geophys. Res.* 87, 6569–6589.
- Brachfeld, S.A., Hammer, J., 2006. Rock magnetic and remanence properties of synthetic Fe-rich basalts: Implications for Mars crustal anomalies. *Earth Planet. Sci. Lett.* 248, 599–617.

- Cande, S.C., Kent, D.V., 1995. Revised calibration of the geomagnetic polarity timescale for the late Cretaceous and Cenozoic. *J. Geophys. Res.* 100, 6093–6095.
- Carlut, J., Kent, D.V., 2002. Grain-size-dependent paleointensity results from very recent Mid-Ocean Ridge basalts. *J. Geophys. Res.* 107, 2049 (10.1029/2001JB000439).
- Carmichael, C.M., 1970. The Mid-Atlantic ridge near 45°N. VII. Magnetic properties and mineralogy of dredged samples. *Can. J. Earth Sci.* 7, 239–256.
- Channell, J.E.T., Mazaud, A., Sullivan, P., Turner, S., Raymo, M.E., 2002. Geomagnetic excursions and paleointensities in the Matuyama Chron at Ocean Drilling Program Sites 983 and 984 (Iceland Basin). *J. Geophys. Res.* 107, 2114 (10.1029/2001JB000491).
- Draeger, U., Prévot, M., Poidras, T., Riisager, J., 2006. Single-domain chemical, thermochemical and thermal remanences in a basaltic rock. *Geophys. J. Int.* 166, 12–32.
- Dunlop, D.J., Özdemir, Ö., 1997. *Rock Magnetism*. Cambridge University Press, p. 573.
- Dunlop, D.J., Xu, S., Heider, F., 2004. Alternating field demagnetization, single-domain-like memory, and the Lowrie-Fuller test of multidomain magnetite grains (0.6–356 µm). *J. Geophys. Res.* 109, B07102 (doi:10.1029/2004JB003006).
- Fridleifsson, I.B., 1973. Petrology and structure of the Esja Quaternary volcanic region. D. Phil. University of Oxford, SW-Iceland, p. 208.
- Fridleifsson, I.B., Kristjansson, L., 1972. The Stardalur Magnetic Anomaly, vol. 22. Jökull, SW-Iceland, pp. 69–78.
- Fridleifsson, I.B., Tomasson, J., 1972. *Jardhitarannsóknir á Stardalssvaedinu 1969–1971*. Mimeographed Report. Orkustofnun, Reykjavik, 14 pp.
- Gee, J., Kent, D.V., 1997. Magnetization of axial lavas from the southern East Pacific Rise (14°–23°S): geochemical controls on magnetic properties. *J. Geophys. Res.* 102, 24873–24886.
- Gee, J., Schneider, D.A., Kent, D.V., 1996. Marine magnetic anomalies as recorders of geomagnetic intensity variations. *Earth Planet. Sci. Lett.* 144, 327–335.
- Griffiths, R.W., Fink, J.H., 1992. Solidification and morphology of submarine lavas: a dependence on extrusion rate. *J. Geophys. Res.* 97, 19729–19737.
- Gunnlaugsson, H.P., Weyer, G., Helgason, Ö., 2002. Titanomaghemite in Icelandic basalt: possible clues for the strongly magnetic phase in Martian soil and dust. *Planet. Space Sci.* 50, 157–161.
- Gunnlaugsson, H.P., Bendtsen, L.S., Bertelsen, P., Binau, C.S., Gaarsmand, J., Goetz, W., Helgason, Ö., Kristjánsson, L., Knudsen, J.M., Leer, K., Madsen, M.B., Nørnberg, P., Steinbórsson, S., Weyer, G., 2003. Magnetic Anomalies in Iceland: Implications for the Magnetic Anomalies on Mars. Sixth International Conference on Mars, Pasadena (Abstract no. 3025).
- Gunnlaugsson, H.P., Helgason, Ö., Kristjánsson, L., Nørnberg, P., Rasmussen, H., Steinthorsson, S., Weyer, G., 2006. Magnetic properties of olivine basalt: application to Mars. *Phys. Earth Planet. Interiors* 154, 276–289.
- Haggerty, S.E., 1991. Oxide textures—a mini-atlas. In: Lindsley, D.H. (Ed.), *Oxide Minerals: Petrologic and Magnetic Significance*, vol. 25. Mineralogical Society of America, pp. 129–219 (Reviews in Mineralogy).
- Haggerty, S.E., Baker, I., 1967. The alteration of olivine in basaltic and associated lavas. Part I. High temperature alteration. *Contribut. Miner. Petrol.* 16, 233–257.
- Haigh, G., 1958. The process of magnetization by chemical change. *Philos. Mag.* 3, 267–286.
- Hall, J.M., 1985. The Iceland Research Drilling Project crustal section: variation of magnetic properties with depth in Icelandic-type oceanic crust. *Can. J. Earth Sci.* 22, 85–101.
- Helgason, Ö., Steinthorsson, S., Madsen, M.B., Mørup, S., 1990. On anomalously magnetic basalt lavas from Stardalur, Iceland. *Hyperfine Interact.* 57, 2209–2214.
- Helgason, Ö., Gunnlaugsson, H.P., Steinthorsson, S., Mørup, S., 1992. High temperature stability of maghemite in partially oxidized basalt lava. *Hyperfine Interact.* 70, 981–984.
- Hunt, C.P., Moskowitz, B.M., Banerjee, S.K., 1995. Magnetic properties of rocks and minerals. In: Ahrens, T.J. (Ed.), *AGU Reference Shelf 3—Rock Physics and Phase Relations. A Handbook of Physical Constants*, pp. 189–204.
- Jakobsson, S.P., Jonsson, J., Shido, F., 1978. Petrology of the Western Reykjanes Peninsula, Iceland. *J. Petrol.* 19, 669–705.
- Jonsson, G., Kristjansson, L., Sverrisson, M., 1991. Magnetic surveys of Iceland. *Tectonophysics* 189, 229–247.
- Kakol, Z., Honig, J.M., 1989. The variation of Verwey transition temperature with oxygen stoichiometry in magnetite. *Solid State Commun.* 70, 967–969.
- Keefer, C.M., Shive, P.N., 1980. Titanomaghemites: conditions for oxidation, influence of rhombohedral phases, and temperature of inversion. *Earth Planet. Sci. Lett.* 51, 199–205.
- Kletetschka, G., Kontny, A., 2005. Identification of magnetic minerals by scanning electron microscope and application of ferrofluid. *Stud. Geophys. Geodaetica* 49, 153–162.
- Kobayashi, K., 1959. Chemical remanent magnetization of ferromagnetic minerals and its application to rock magnetism. *J. Geomagn. Geoelectr.* 10, 99–117.
- Kontny, A., Vahle, C., de Wall, H., 2003. Characteristic magnetic behavior of subaerial and submarine lava units from the Hawaiian Scientific Drilling Project (HSDP-2). *Geochem. Geophys. Geosyst.* 4, 8703 (doi:10.1029/2002GC000304).
- Kristjansson, L., 1970. Palaeomagnetism and magnetic surveys in Iceland. *Earth Planet. Sci. Lett.* 8, 101–108.
- Kristjansson, L., 1985. Magnetic and thermal effects of dike intrusions in Iceland. *J. Geophys. Res.* 90, 10129–10135.
- Kristjansson, L., Fridleifsson, I.B., Watkins, N.D., 1980. Stratigraphy and paleomagnetism of the Esja, Eyrafjall and Akrafjall Mountains, SW-Iceland. *J. Geophys.* 47, 31–42.
- Lattard, D., Engelmann, R., Kontny, A., Sauerzapf, U., 2006. Curie temperatures of synthetic titanomagnetites in the Fe-Ti-O system: effects of composition, crystal chemistry and thermomagnetic methods. *J. Geophys. Res.* 111 (B12), doi:10.1029/2006JB004591.
- Lowrie, W., 1990. Identification of ferromagnetic minerals in a rock by coercivity and unblocking temperature properties. *Geophys. Res. Lett.* 17, 159–162.
- Matzka, J., Krása, D., Kunzmann, T., Schult, A., Petersen, N., 2003. Magnetic state of 10–40 Ma old ocean basalts and its implications for natural remanent magnetization. *Earth Planet. Sci. Lett.* 206, 541–553.
- Meynadier, L., Valet, J.-P., Shackleton, N.J., 1995. Relative geomagnetic intensity during the last 4 m.y. from the equatorial Pacific. In: *Proceedings of the Ocean Drilling Program, Scientific Results*, vol. 138, pp. 779–795.
- Moskowitz, B.M., Jackson, M., Kissel, C., 1998. Low-temperature magnetic behavior of titanomagnetites. *Earth Planet. Sci. Lett.* 157, 141–149.
- Murad, E., 1996. Magnetic properties of microcrystalline iron (III) oxides and related materials as reflected in their Mössbauer spectra. *Phys. Chem. Miner.* 23, 248–262.

- Muxworthy, A.R., McClelland, E., 2000. Review of the low-temperature magnetic properties of magnetite from a rock magnetic perspective. *Geophys. J. Int.* 140, 101–114.
- O'Reilly, W., 1983. The identification of titanomaghemites: model mechanisms for the maghemitization and inversion processes and their magnetic consequences. *Phys. Earth Planet. Interiors* 31, 65–76.
- Özdemir, Ö., Dunlop, D.J., 1997. Effect of crystal defects and internal stresses on the domain structure and magnetic properties of magnetite. *J. Geophys. Res.* 102, 20211–20224.
- Özdemir, Ö., Dunlop, D.J., 1998. Single-domain-like behavior in a 3-mm natural single crystal of magnetite. *J. Geophys. Res.* 103(B2), 2549–2562.
- Özdemir, Ö., Dunlop, D.J., Moskowitz, B.M., 1993. The effect of oxidation on the Verwey transition in magnetite. *Geophys. Res. Lett.* 20, 1671–1674.
- Petersen, N., Vali, H., 1987. Observation of shrinkage cracks in ocean floor titanomagnetites. *Phys. Earth Planet. Interiors* 46, 197–205.
- Petrovsky, E., Kapicka, A., 2005. Comments on “The use of field dependence of magnetic susceptibility for monitoring variations in titanomagnetite composition - a case study on basanites from the Vogelsberg 1996 drillhole, Germany” by de Wall and Nano. In: *Stud. Geophys. Geodaetica*. 48, 767–776. *Stud. Geophys. Geodaetica*, 49, 255–258.
- Pouchon, J.L., Pichoir, F., 1984. A new model for quantitative X-ray microanalysis. Part I. Application to the analysis of homogeneous samples. *La Recherche Aérospatiale* 3, 167–192.
- Purucker, M., Ravat, D., Frey, H., Voorhies, C., Sabaka, T., Acuña, M.H., 2000. An altitude-normalized magnetic map of Mars and its interpretation. *Geophys. Res. Lett.* 27, 2449–2452.
- Rhodes, J.M., Vollinger, M.J., 2004. Composition of basaltic lavas sampled by phase-2 of the Hawaiian Scientific Drilling Project: geochemical stratigraphy and magma types. *Geochem. Geophys. Geosyst.* 5, Q03G13, doi:10.1029/2002GC000434.
- Smith, P.J., 1967. The intensity of the Tertiary geomagnetic field. *Geophys. J. R. Astronom. Soc.* 12, 239–258.
- Steinþorsson, S., Sigvaldason, G.E., 1971. *Skýrsla um bergfræðirannsóknir við Stardal*. Report. Science Institute, University of Iceland.
- Steinþorsson, S., Helgason, Ö., Madsen, M.B., Koch, C.B., Bentzon, M.D., Morup, S., 1992. Maghemite in Icelandic basalts. *Mineral. Mag.* 56, 185–199.
- Stolper, E.M., Sherman, S., Garcia, M., Baker, M., Seaman, C., 2004. Glass in the submarine section of the HSDP2 drill core, Hilo, Hawaii. *Geochem. Geophys. Geosyst.* 5, Q07G15, doi:10.1029/2003GC000553.
- Vahle, C., 2005. *Aufbau und Entwicklung des Vulkans Mauna Kea anhand von gesteinsmagnetischen und magneto-mineralogischen Untersuchungen an Kernen des “Hawaii Scientific Drilling Project” (HSDP-2)*. Inaugural-Dissertation zur Erlangung der Doktorwürde, Naturwissenschaftlich-Mathematische Gesamtfakultät. Ruprecht-Karls-Universität Heidelberg, p. 285.
- Verwey, E.J.W., 1939. Electronic conduction of magnetite (Fe_3O_4) and its transition point at low temperatures. *Nature* 144, 327–328.
- Wang, D., Van der Voo, R., Peacor, D.R., 2005. Why is the remanent magnetic intensity of Cretaceous MORB so much higher than that of mid to late Cenozoic MORB? *Geosphere* 1, 138–146.
- Yamazaki, T., Oda, H., 2005. A geomagnetic paleointensity stack between 0.8 and 3.0 Ma from equatorial Pacific sediment cores. *Geochem. Geophys. Geosyst.* 6, Q11H20, doi:10.1029/2005BC001001.
- Zhou, W., Van der Voo, R., Peacor, D.R., Zhang, Y., 2000. Variable Ti-content and grain size of titanomagnetite as a function of cooling rate in very young MORB. *Earth Planet. Sci. Lett.* 179, 9–20.